

1971

I. The low temperature photochemistry of iron pentacarbonyl and disubstituted acetylenes, II. The X-ray structure determination of trans-6,8-dibromo-1,2,3,4,4a,9a-hexahydro-4a,9-dimethylcarbazole

Allen Bloom
Iowa State University

Follow this and additional works at: <https://lib.dr.iastate.edu/rtd>

 Part of the [Organic Chemistry Commons](#)

Recommended Citation

Bloom, Allen, "I. The low temperature photochemistry of iron pentacarbonyl and disubstituted acetylenes, II. The X-ray structure determination of trans-6,8-dibromo-1,2,3,4,4a,9a-hexahydro-4a,9-dimethylcarbazole " (1971). *Retrospective Theses and Dissertations*. 4943.

<https://lib.dr.iastate.edu/rtd/4943>

This Dissertation is brought to you for free and open access by the Iowa State University Capstones, Theses and Dissertations at Iowa State University Digital Repository. It has been accepted for inclusion in Retrospective Theses and Dissertations by an authorized administrator of Iowa State University Digital Repository. For more information, please contact digirep@iastate.edu.

72-5178

BLOOM, Allen, 1943-

I. THE LOW TEMPERATURE PHOTOCHEMISTRY OF IRON
PENTACARBONYL AND DISUBSTITUTED ACETYLENES.

II. THE X-RAY STRUCTURE DETERMINATION OF trans-
6,8,-DIBROMO-1,2,3,4,4a,9a-HEXAHYDRO-4a,9-
DIMETHYLCARBAZOLE.

Iowa State University, Ph.D., 1971
Chemistry, organic

University Microfilms, A XEROX Company, Ann Arbor, Michigan

I. The low temperature photochemistry of iron
pentacarbonyl and disubstituted acetylenes
II. The X-ray structure determination of trans-6,8-
dibromo-1,2,3,4,4a,9a-hexahydro-4a,9-dimethylcarbazole

By

Allen Bloom

A Dissertation Submitted to the
Graduate Faculty in Partial Fulfillment of
The Requirements for the Degree of

DOCTOR OF PHILOSOPHY

Major Subject: Organic Chemistry

Approved:

Signature was redacted for privacy.

In Charge of Major Work

Signature was redacted for privacy.

Head of Major Department

Signature was redacted for privacy.

Dean of Graduate College

Iowa State University
Of Science and Technology
Ames, Iowa

1971

PLEASE NOTE:

Some Pages have indistinct
print. Filmed as received.

UNIVERSITY MICROFILMS

TABLE OF CONTENTS

	Page
PART I. THE LOW TEMPERATURE PHOTOCHEMISTRY OF IRON PENTACARBONYL AND DISUBSTITUTED ACETYLENES	1
INTRODUCTION	2
REVIEW OF THE LITERATURE	3
RESULTS AND DISCUSSION	10
Iron Pentacarbonyl	10
Iron Pentacarbonyl and 3-Hexyne	23
Iron Pentacarbonyl and Diphenylacetylene	42
Diphenylacetylene	55
EXPERIMENTAL	60
General	60
Low Temperature Experiments	60
Method A	60
Method B	61
Iron pentacarbonyl	62
Iron pentacarbonyl and 3-hexyne	63
Iron pentacarbonyl and diphenylacetylene	65
Diphenylacetylene	66
PART II. THE X-RAY STRUCTURE DETERMINATION OF <u>TRANS</u> -6,8- DIBROMO-1,2,3,4,4a,9a-HEXAHYDRO-4a,9- DIMETHYLCARBAZOLE	68
INTRODUCTION	69
EXPERIMENTAL	70
DISCUSSION	78
LITERATURE CITED	80
ACKNOWLEDGMENTS	84
APPENDIX	85
VITA	93

PART I. THE LOW TEMPERATURE PHOTOCHEMISTRY OF IRON
PENTACARBONYL AND DISUBSTITUTED ACETYLENES

INTRODUCTION

Photochemistry and organometallic chemistry are on the borders of several traditional chemical disciplines. These areas have attracted the interest of chemists from varied backgrounds and have led to explosive activity and many novel and challenging problems.

This study is concerned with the investigation of the interaction of iron pentacarbonyl and diphenyl- and diethylacetylene. The primary tool is infrared spectroscopy and the heart of the technique is the cooling of the starting material to cryoscopic temperatures followed by irradiation of the sample with ultraviolet light at the low temperatures. The object is to separate photo-initiated reactions from thermally induced reactions.

REVIEW OF THE LITERATURE

Iron pentacarbonyl was first prepared (1, 2) by passing a stream of carbon monoxide over iron filings. It is a volatile liquid sensitive to light and air. Mossbauer (3), Raman (4), and infrared (5-9) spectroscopy as well as X-ray (10, 11) and electron diffraction (12-18) structure determination all confirm the D_{3h} trigonal bipyramidal structure. Some controversy exists (14-16) over the accuracy of electron diffraction methods as compared to X-ray diffraction methods. The latest results for each method (11, 18) are reported below.

Table 1. $Fe(CO)_5$ bond lengths

Diffraction Method	Fe-C (axial)	Fe-C (equa.)	C-O (mean)
X-ray	$1.810 \pm 0.020 \text{ \AA}$	$1.797 \pm 0.017 \text{ \AA}^a$ $1.763 \pm 0.034 \text{ \AA}^b$	$1.10 - 1.14 \text{ \AA}$
electron	1.832^c	$1.832 \pm 0.000 -$ $.050$	1.147 ± 0.002^a

^aTwo equatorial positions are identical in the structure.

^bNon-identical equatorial position.

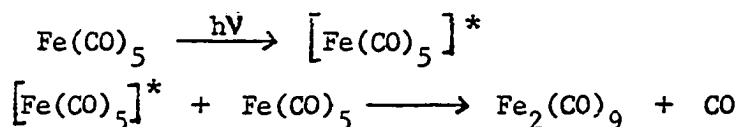
^cMean Fe-C distance of all five bonds.

The electron diffraction results generally show the axial Fe-C bond length to be shorter than the equatorial, while the X-ray work shows the opposite. Schreiner and Brown (19) have performed molecular orbital calculations which indicate the axial Fe-C bond dissociation energy to

be 89 kcal/mole. This is slightly less than the corresponding equatorial bond.

Nmr experiments (20, 21) show that all five $^{13}\text{C-O}$ are equivalent and that pseudorotation (22) is probably occurring. No intermolecular exchange occurs in the dark (23, 24) although rapid, non-specific exchange (24, 25) occurs on irradiation. The fact that the infrared spectra show the expected bands for D_{3h} symmetry while the nmr is a singlet indicates that the rate of pseudorotation lies between these two time scales, 1.0×10^{-8} sec (ir) to 1.0×10^{-2} sec (nmr). $\text{Fe}(\text{PF}_3)_5$ has also been shown (26) to undergo pseudorotation.

Iron pentacarbonyl is extremely reactive to ultraviolet light. Dewar and Jones (27) found that 2 $\text{Fe}(\text{CO})_5$ were consumed for each $\text{Fe}_2(\text{CO})_9$ molecule formed. Later work (28) confirmed the earlier observations and showed that adding CO , H_2 , Ar , etc., did not affect the gas phase reaction. Keeley and Johnson (24) irradiated $\text{Fe}(\text{CO})_5$ over an atmosphere of ^{14}CO and found rapid, non-specific incorporation in the recovered $\text{Fe}(\text{CO})_5$, but very little in the $\text{Fe}_2(\text{CO})_9$ which formed. They concluded that $\text{Fe}(\text{CO})_4$ was not an intermediate in $\text{Fe}_2(\text{CO})_9$ formation because of the low incorporation and proposed the following mechanism:

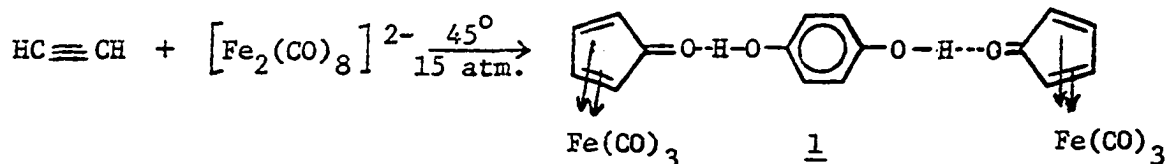


Recently, however, Noack and Ruch (25) restudied the photolysis of $\text{Fe}(\text{CO})_5$ using C^{18}O and ^{13}CO . They obtained essentially the same results, but found their experiments consistent with the intermediacy of $\text{Fe}(\text{CO})_4$

rather than the Keeley-Johnson mechanism.

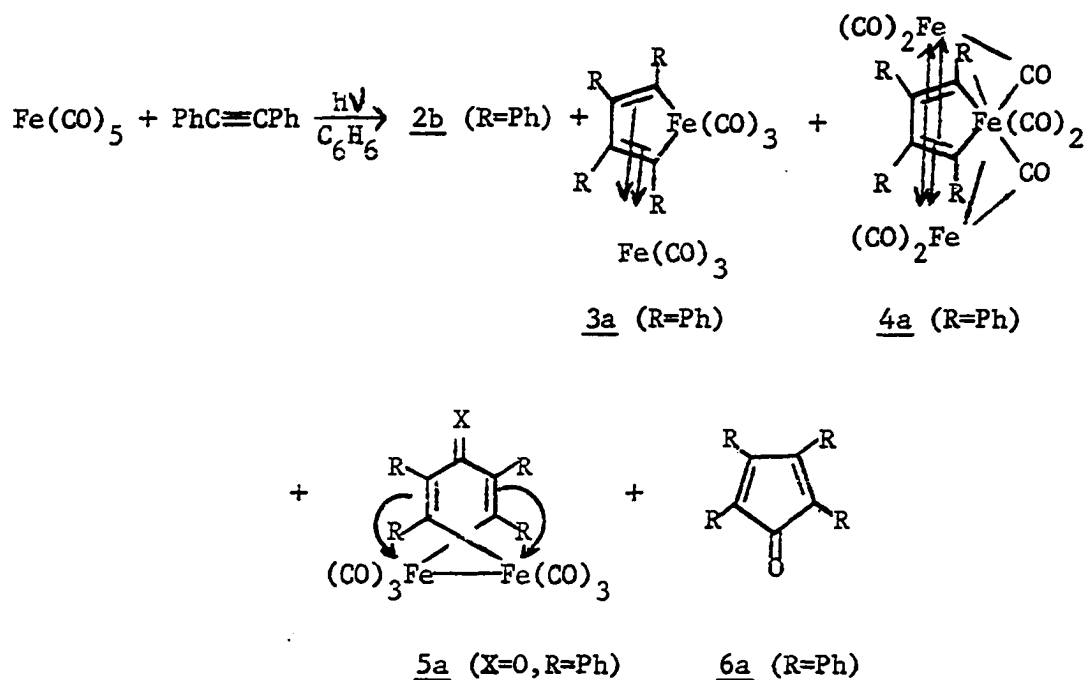
Sheline and coworkers (29) irradiated $\text{Fe}(\text{CO})_5$ in 1:4 methylcyclohexane-isopentane (MCIP) glass in a quartz tube cooled with liquid nitrogen. The tube was melted following irradiation and the infrared spectrum revealed a single, new band at 1834 cm^{-1} . In later work (30), the infrared spectrum following irradiation was taken without melting the tube and new bands were observed at 1990 (s), 1980 (w), and 1946 (s) cm^{-1} with no band at 1834 cm^{-1} .

The chemistry of iron carbonyls with acetylenes is very complex, and often gives rise to spectacular products. Reviews on this work have recently appeared (31, 32). Much of the structural work which was speculated on by workers in the field has subsequently been shown to be wrong by X-ray analysis and in the discussion which follows only the currently accepted structure will be used. Modern interest in the field stems from the work of Reppe (33) carried out during and immediately after the second world war. By reacting acetylene with $[\text{Fe}_2(\text{CO})_8]^{2-}$ (33-35) a compound (1) of the composition

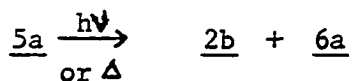


" $\text{FeC}_{11}\text{H}_7\text{O}_5$ " was formed which in dilute acid or hot water formed hydroquinone and a compound shown to be cyclopentadieneonetricarbonyliron (2a)

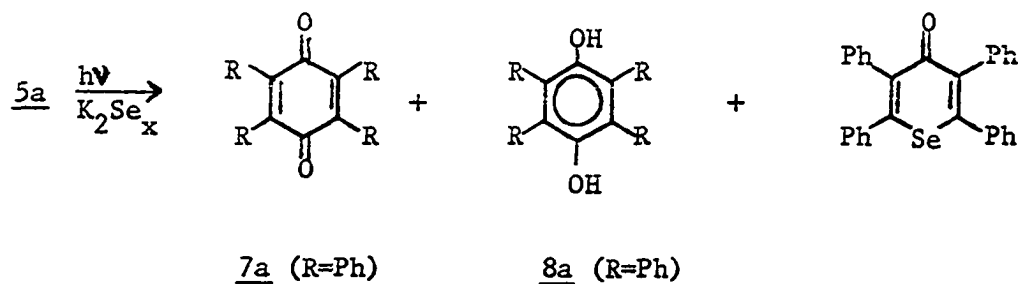
Schrauzer (36) irradiated $\text{Fe}(\text{CO})_5$ with diphenylacetylene in refluxing benzene and isolated five compounds.



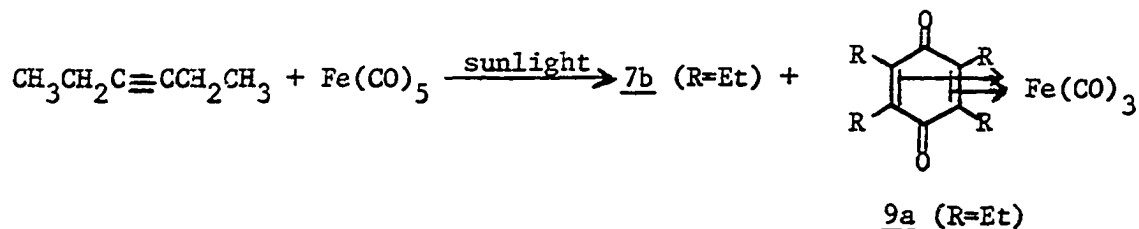
If the reaction was interrupted during the early stages only 5a was isolated, and when heated 2b was obtained. It has now been shown (37) 2b and 6a can be isolated when 5a is reacted thermally or photochemically.



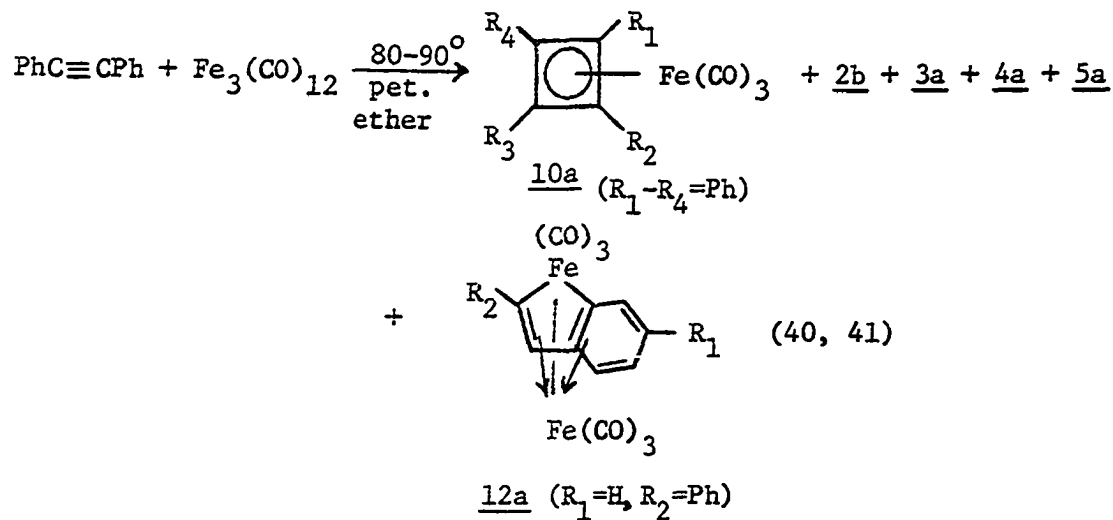
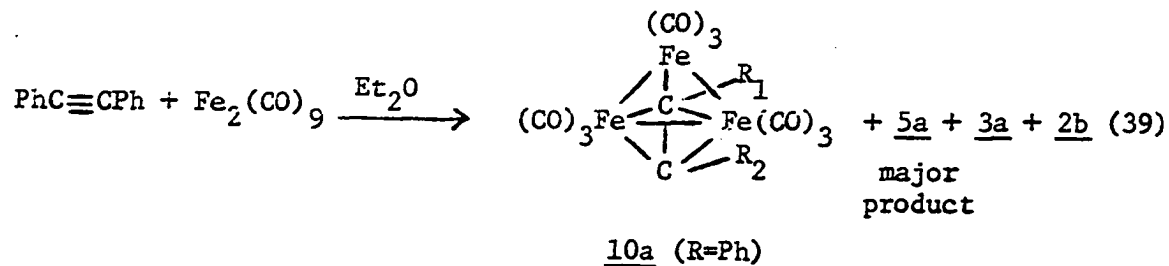
Also, if 5a is irradiated in the presence of potassium polyselenide tetraphenyl-p-benzoquinone (7a) and tetraphenylhydroquinone (8a) are isolated in 95% yield along with tetraphenyl 2-selapyrone.



When various aliphatic alkynes were exposed to sunlight in inert solvents quinone and quinonetricarbonyliron compounds were obtained (38).



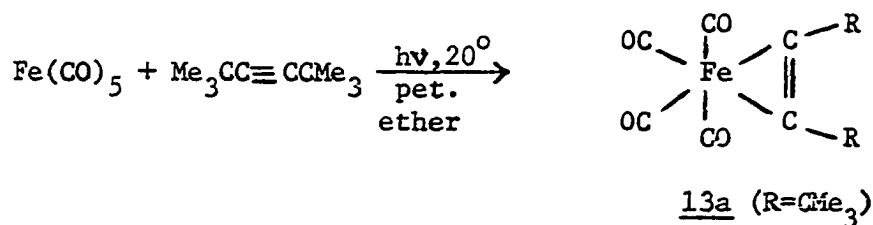
A large volume of work has involved the exploratory and structural (31, 32) aspects of the thermal reactions of iron carbonyls with acetylenes.



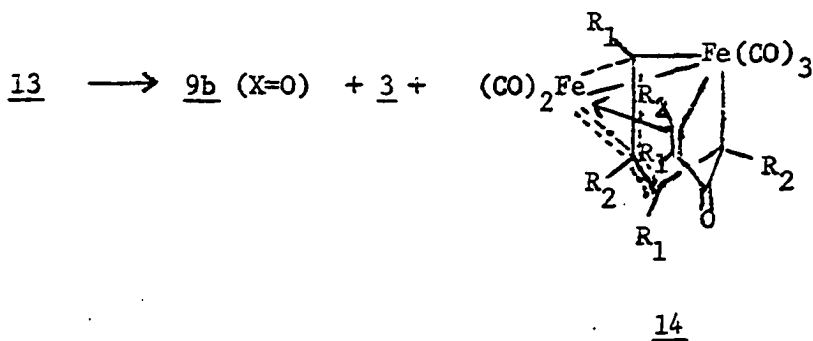
Other workers have studied the reactions of iron carbonyls with fluorinated acetylenes (42-44), acetylene (45), diferrocenylacetylene (46), methylphenylacetylene (39, 47), phenylacetylene (40, 48) and methyl

phenylacetylenecarboxylate (49) among others. These reactions often led to new organoiron compounds.

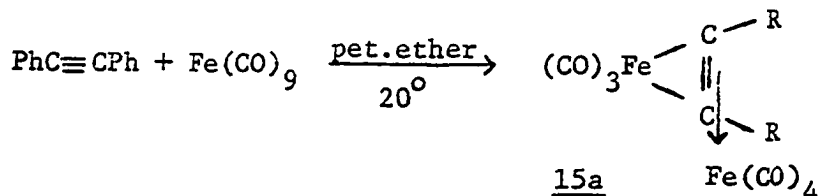
When acetylenes containing bulky groups are irradiated at 20°C, simple complexes of the formula $(RC\equiv CR_1)Fe(CO)_4$ (13) can be isolated (50) with the acetylene coordinated in the equatorial position. On warming, these compounds form typical products of iron carbonyl-acetylene



reactions.

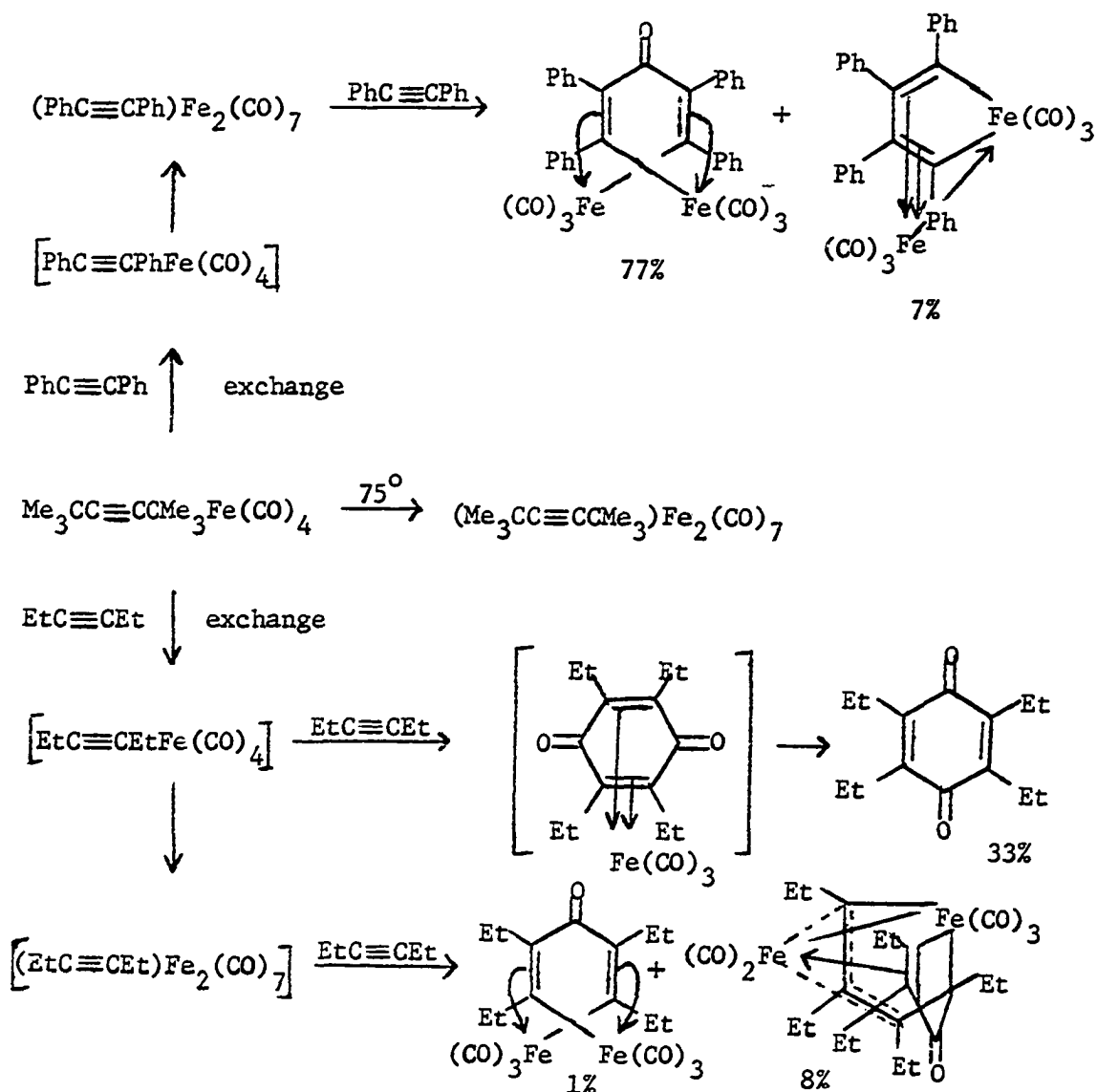


When iron nonacarbonyl is reacted with diphenylacetylene (50) under carefully controlled conditions $(PhC\equiv CPh)Fe_2(CO)_7$ (15a) is isolated.

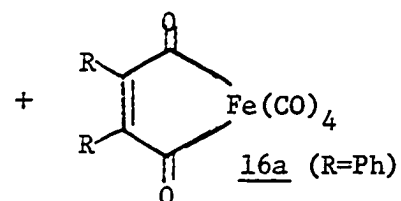
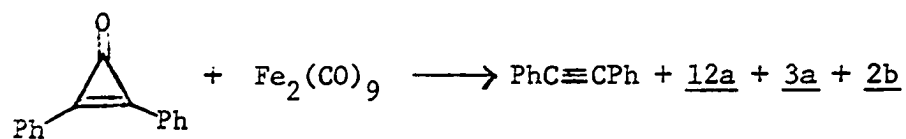
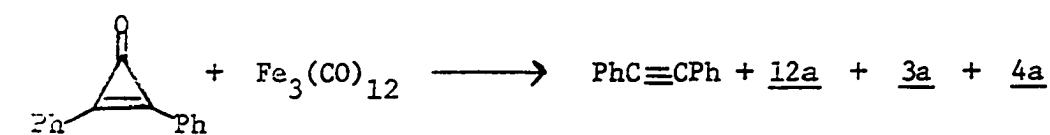


Both 13 and 15 have been shown to be key intermediates in iron carbonyl-acetylene reactions.

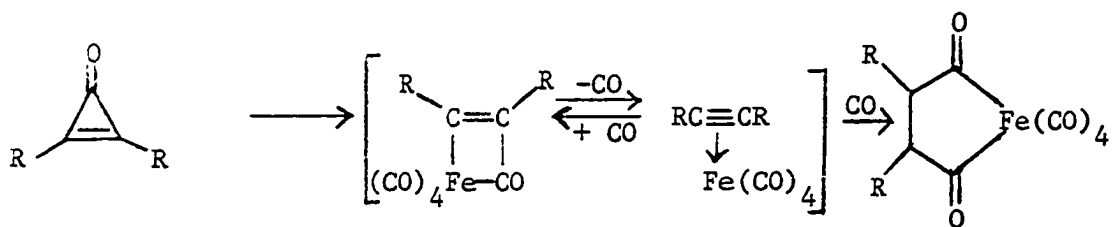
Hübel (51) has presented the following scheme to explain some of the observed organoiron compounds on interaction of acetylenes with iron carbonyls:



In related work (52) diphenylcyclopropenone was reacted with various iron carbonyls to yield many products in common with those from diphenylacetylene-iron carbonyl reactions.



The postulated mechanism involves $\text{Fe}(\text{CO})_4$ insertion followed by CO loss and rearrangement.



RESULTS AND DISCUSSION

Iron Pentacarbonyl

Figure 1 shows the infrared spectrum of iron pentacarbonyl recorded at 77°K^1 as a neat film between sodium chloride plates fitted with an 0.007 mm, aluminum spacer. Bands were observed at 2113 (vw)², 2074 (m), 2034 (sh), 1994 (sh), 1985 (s), 1948 (ms), 1813 (w,br), 641 (sh) and 630 (s) cm^{-1} .

Upon irradiation using a Pyrex filter new bands appeared at 2138 (w) and 1955 (ms) cm^{-1} . In addition the 1985 cm^{-1} band showed some broadening. Figure 2 depicts the infrared spectrum recorded after irradiation for 146 minutes.

The low temperature unit was then slowly warmed. As the temperature increased, the bands at 1955 cm^{-1} began to diminish with concomitant formation of bands at 1818 and 1827 cm^{-1} . The 2138 cm^{-1} band also decreased. After warming to 252°K , the unit was rapidly cooled to 77°K and the recorded infrared spectrum is reproduced in Figure 3. The band at 1955 cm^{-1} disappeared, the 1985 cm^{-1} band sharpened and the 2138 cm^{-1} band was virtually gone. The new bands at 1827 (wm) and 1818 (wm) cm^{-1} can also be seen.

¹ The accuracy of temperature measurement is probably no better than $\pm 10^{\circ}$.

² The shorthand employed for describing the infrared bands is w = weak, m = medium, s = strong, v = very, sh = shoulder and br = broad.

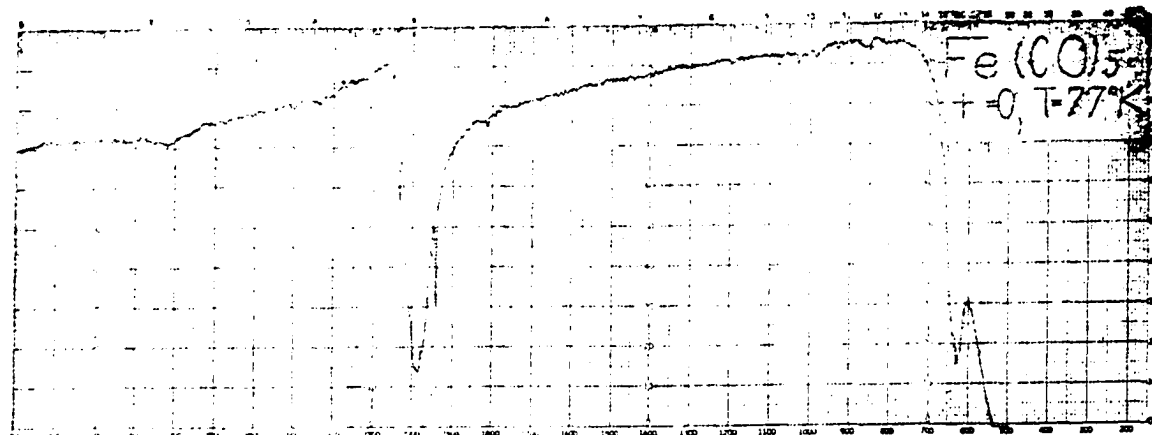


Figure 1. Iron pentacarbonyl at 77°K

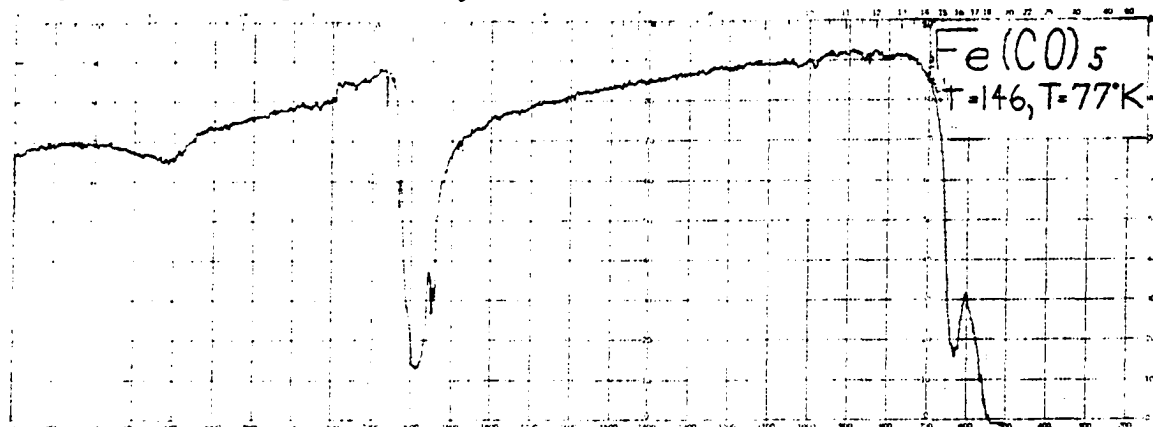


Figure 2. Iron pentacarbonyl at 77°K after irradiation for 146 min.

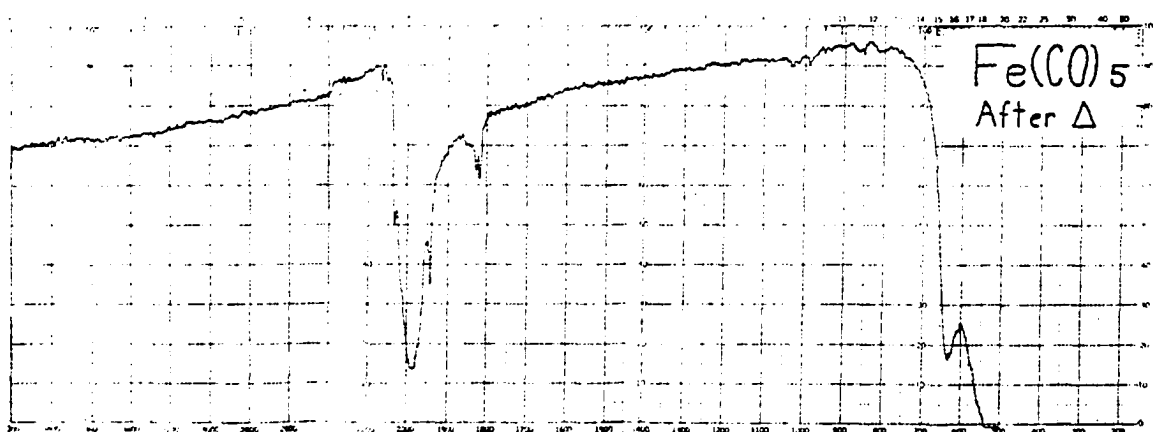


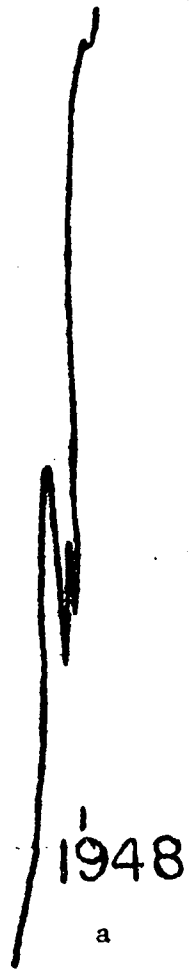
Figure 3. Iron pentacarbonyl at 77°K after warmup

Figures 4-6 focus on selected bands during the course of the reaction. In Figure 4, the disappearance of the 1955 cm^{-1} during warmup is shown. By 242°K all remnants of this band is gone while the band at 1949 cm^{-1} band remains. Figure 5 records the formation of the bands at 1818 and 1827 cm^{-1} during warmup. The 1818 cm^{-1} band appears as the stronger of the two. Finally, Figure 6 shows the disappearance of the 2138 cm^{-1} band associated with carbon monoxide during warmup. As the temperature increases, the carbon monoxide is able to diffuse more rapidly out of the matrix.

Room temperature infrared spectra of $\text{Fe}_2(\text{CO})_9$ and $\text{Fe}_3(\text{CO})_{12}$ in KBr pellets were obtained. For $\text{Fe}_2(\text{CO})_9$ bands occurred at 2077 (m), 2014 (s), 1984 (sh) and 1827 (m) cm^{-1} as can be seen in Figure 7, while bands occurred at 2041 (s), 2008 (s), 1919 (sh), 1855 (w) and 1828 (w) cm^{-1} for $\text{Fe}_3(\text{CO})_{12}$ as seen in Figure 8. Further, $\text{Fe}_2(\text{CO})_9$ suspended in $\text{Fe}(\text{CO})_5$ at 77°K (see Figure 9) has bands at 1820 (ms), 1948 (sh), 1952 (sh), 1998 (s), 2012 (ms), 2022 (ms) and 2076 (sh) cm^{-1} . An $\text{Fe}_3(\text{CO})_{12} - \text{Fe}(\text{CO})_5$ frozen solution at 77°K , (see Figure 10) had bands at 1820 (w), 1858 (w), 1947 (ms), 1987 (vs), 1992 (vs), 1995 (vs), 2008 (vs), 2037 (s), 2109 (vw) cm^{-1} .

Iron contains 26 electrons and in its coordination compounds tries to obtain the necessary 10 electrons to yield a rare gas configuration. Carbon monoxide is a two electron donor, donating the non-bonding sp electron pair on the carbon atom. The additional electron density on the iron atom is redistributed back to the carbon monoxide by means of back donation of the appropriate d orbitals of the iron to the two

Figure 4. 1900-2000 cm^{-1} region during irradiation, a = 163°K, b = 196°K, c = 216°K, d = 230°K,
e = 242°K



1955

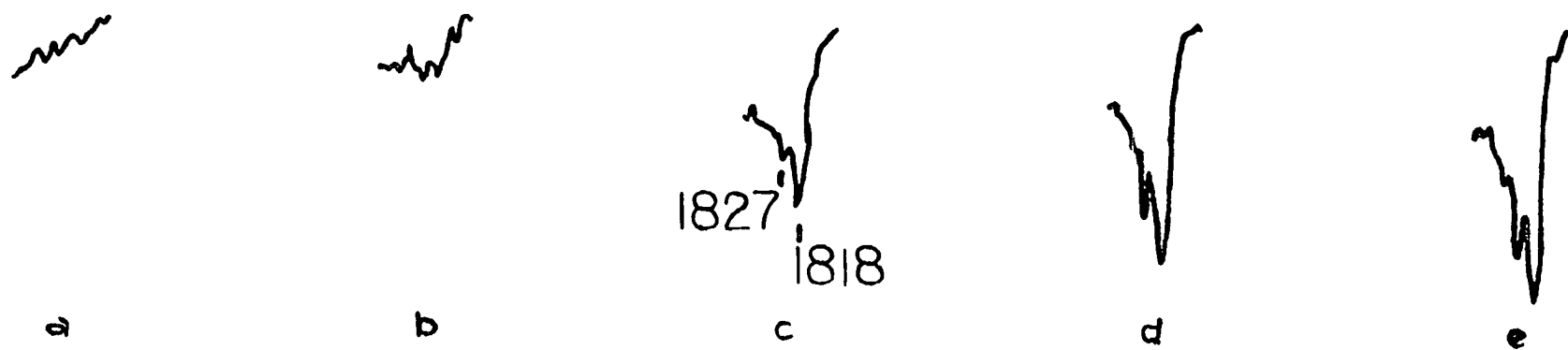


Figure 5. 1800-1850 cm⁻¹ region during warmup, a = 163°K; b = 196°K; c = 216°K; d = 230°K; e = 242°K

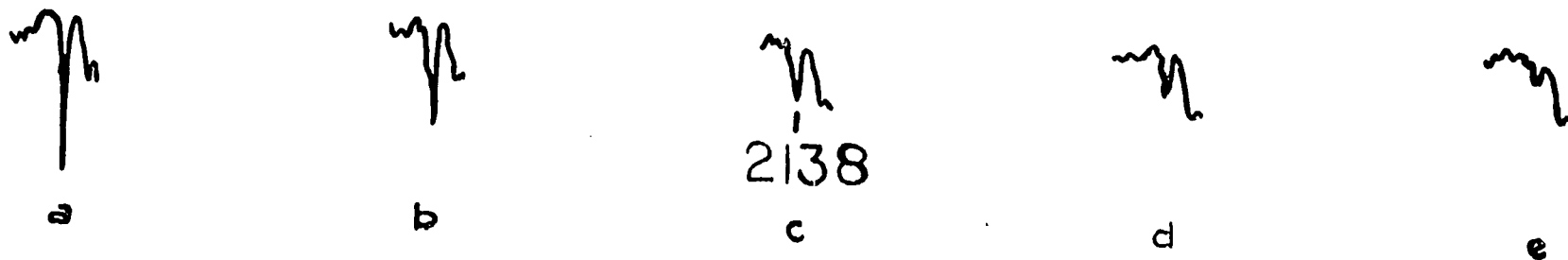


Figure 6. 2100-2200 cm^{-1} region during warmup, a = 163 $^{\circ}$ K; b = 196 $^{\circ}$ K; c = 216 $^{\circ}$ K; d = 230 $^{\circ}$ K; e = 242 $^{\circ}$ K

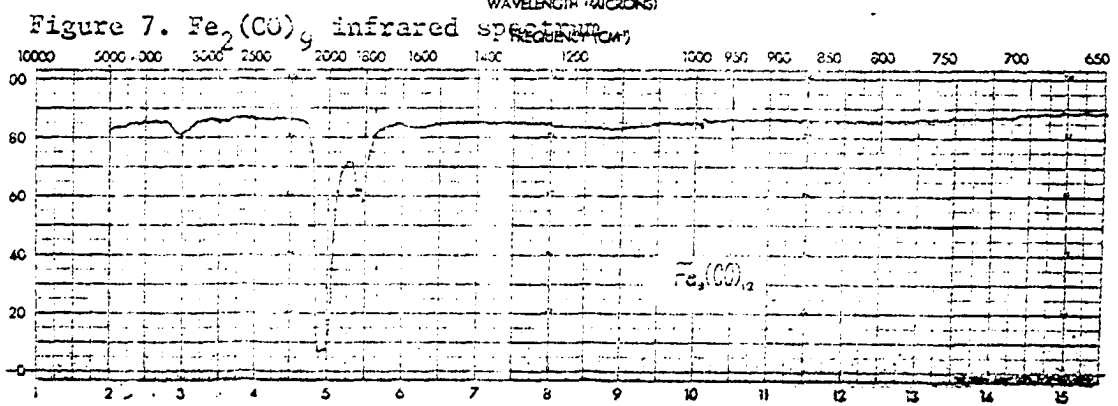
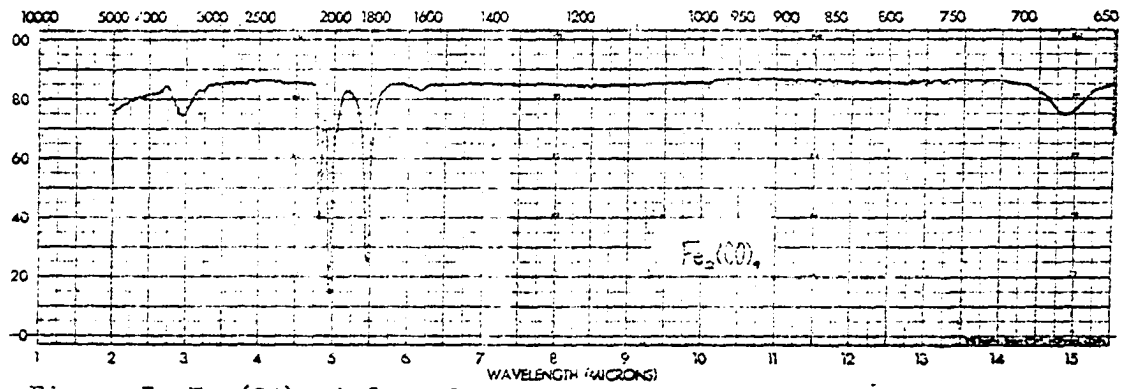


Figure 8. $\text{Fe}_3(\text{CO})_{12}$ infrared spectrum

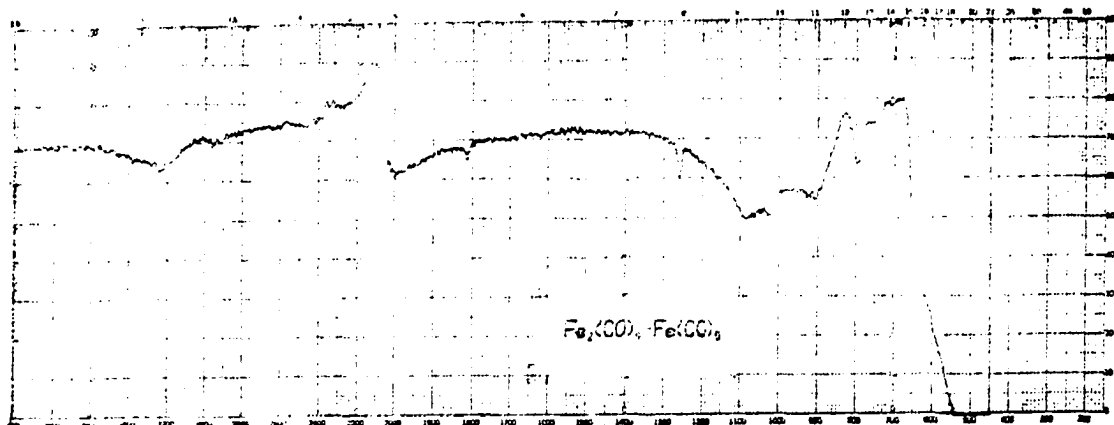


Figure 9. $\text{Fe}_2(\text{CO})_9 - \text{Fe}(\text{CO})_5$ at 77°K

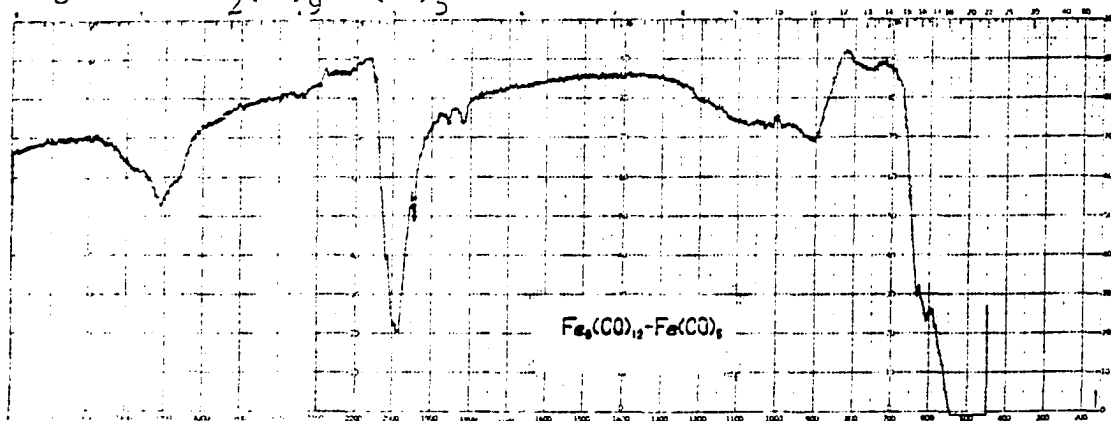


Figure 10. $\text{Fe}_3(\text{CO})_{12} - \text{Fe}(\text{CO})_5$ at 77°K

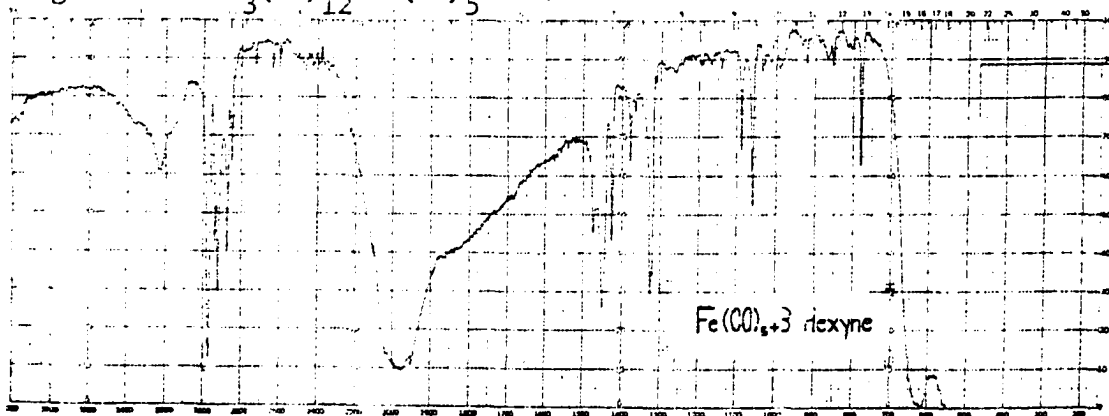


Figure 11. First run of $\text{Fe}(\text{CO})_5 + 3\text{-hexyne}$ before irradiation

orbitals of the carbon monoxide. The details of the bonding in $\text{Fe}(\text{CO})_5$ have recently been discussed by Brown (19).

Table 2 below compares the infrared bands observed on cooling $\text{Fe}(\text{CO})_5$ to 77°K with the results and assignments obtained by several laboratories, codified and reported by Jones and McDowell (7).

Table 2. Assignment and comparison of $\text{Fe}(\text{CO})_5$ infrared bands

This work	Jones and McDowell ^a	Assignment
2113	2114 ^b	$\nu_6 + \nu_{18}$
2074	2086	$\nu_{10} + \nu_{15}$
2034	2031	ν_2
1994	2009	ν_6
1985	1984	ν_{10}
1948	1946	$\nu_{\text{C}^{13}-\text{O}}$
641	644	ν_{11}
630	620	ν_7

^aSee reference 7.

^bAll bands were recorded in the liquid phase at room temperature except those in the 600 cm^{-1} region which was recorded in the solid (7, 8) at 77°K .

In general there is good agreement between the low temperature spectrum and those of others in the liquid phase. The 2074 and 1994 cm^{-1} bands are shifted to lower frequency from the corresponding solution.

bands. The quite weak band at 1813 cm^{-1} may be due to solid state effects or impurity.

The new band at 1955 cm^{-1} as well as the broadening of the 1985 cm^{-1} region following irradiation can be explained by invoking an $\text{Fe}(\text{CO})_4$ species. The existence of this compound has been postulated by Orgel (53) among others to explain iron carbonyl chemistry with various ligands. Also, recent isotope replacement experiments of Noack (25) led him to invoke the existence of an $\text{Fe}(\text{CO})_4$ species. The 2138 cm^{-1} is undoubtedly due to free CO in the matrix. Sheline (30) found a CO bond at 2135 cm^{-1} in his irradiation of various metal carbonyls at -180° in an MCIP glass.

The geometry of the $\text{Fe}(\text{CO})_4$ is probably C_{3v} formed by loss of an axial CO. Various light induced ligand and ^{14}C CO replacements (54) have shown that the first step in these reactions is loss of an axial CO in an $\text{S}_{\text{N}}1$ type reaction path. $\text{Fe}(\text{CO})_5$ does not exchange with CO in the dark. Other reasonable four coordinate geometries are regular tetrahedral and square planar which would give rise to only 1 ir active band or a C_{2v} geometry which from loss of an equatorial CO from which one would expect 5 ir active bands. Although one would expect 4 ir active bands from the C_{3v} model, it is possible that either one band is obscured by the $\text{Fe}(\text{CO})_5$ or fortuitous overlap is occurring under the conditions employed.

The results of Sheline and coworkers (29, 30) are germane to our experiments. His early observation of a single band at 1834 cm^{-1} upon irradiation of an $\text{Fe}(\text{CO})_5$ - MCIP glass was changed in his later report to bands at 1990 (s) , 1980 (w) and $1946\text{ (s)}\text{ cm}^{-1}$ and no band at 1834 cm^{-1} . The experimental results reported above support his later report. The

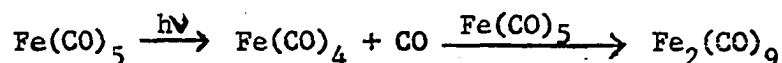
broadening of the band at 1985 cm^{-1} could indicate the formation of bands at 1990 and 1980 cm^{-1} while the band at 1955 cm^{-1} could correspond to his band at 1946 cm^{-1} shifted somewhat by different environments. Both sets of results indicate the presence of a new species upon irradiation, and this species is most probably $\text{Fe}(\text{CO})_4$. No effort was made to maximize the formation of $\text{Fe}(\text{CO})_4$ since Sheline had already performed the experiment. Sheline's (30) low temperature photolysis experiments with other metal carbonyls indicates that loss of CO generally does not lead to further geometric change.

The compound formed on warmup could be $\text{Fe}_2(\text{CO})_9$, $\text{Fe}_3(\text{CO})_{12}$, or the unknown $\text{Fe}_2(\text{CO})_8$. All evidence leaves little doubt that $\text{Fe}_2(\text{CO})_9$ is the species being observed. The gas phase and solution irradiations have long been known to yield $\text{Fe}_2(\text{CO})_9$ (27). The room temperature KBr spectra in Figures 7 and 8 of $\text{Fe}_2(\text{CO})_9$ and $\text{Fe}_3(\text{CO})_{12}$, respectively, clearly show that the 1820 cm^{-1} region is much stronger for $\text{Fe}_2(\text{CO})_9$. In low concentrations the $\text{Fe}_3(\text{CO})_{12}$ bridging bonds would be barely observable. Instead, in the warmup product, they are quite substantial. A mixture of $\text{Fe}_2(\text{CO})_9 - \text{Fe}(\text{CO})_5$ at 77°K as shown in Figure 9 more closely resembles the final spectrum in Figure 3 than does a solution of $\text{Fe}_3(\text{CO})_{12} - \text{Fe}(\text{CO})_5$ at 77°K in Figure 10. The weakness of the spectrum in Figure 8 is due to the insolubility of $\text{Fe}_2(\text{CO})_9$ in $\text{Fe}(\text{CO})_5$ or any other solvent. These spectra make clear the masking of bands of $\text{Fe}_2(\text{CO})_9$.

In the concentration of $\text{Fe}(\text{CO})_4$ present, probably no more than 5-10% of the reaction mixture, a dimerization to form $\text{Fe}_2(\text{CO})_8$ or a trimerization to form $\text{Fe}_3(\text{CO})_{12}$ seems highly unlikely. Previous chemical experiments as well as spectral results presented above rule out the

presence of either of these compounds.

The pathway for the formation of $\text{Fe}_2(\text{CO})_9$ from $\text{Fe}(\text{CO})_5$ is outlined below. $\text{Fe}(\text{CO})_4$ may also be important in the photochemical formation of



$\text{Fe}(\text{CO})_4$ pyridine from $\text{Fe}(\text{CO})_5$ in pyridine (55). Further studies of its chemistry would seem to be warranted.

Iron Pentacarbonyl and 3-Hexyne

This reaction was studied under a variety of conditions. In the first of three runs a 2:1 mixture of 3-hexyne:iron pentacarbonyl was studied at 77°K using an 0.025 mm spacer. The results are summarized in Table 3.

As can be seen in Figure 11, the high $\text{Fe}(\text{CO})_5$ concentration and thick spacer led to a lack of definition in the $1970\text{--}2000\text{ cm}^{-1}$ region. After recording the 320 minute irradiation ir, the photolysis was resumed, but the automatic nitrogen leveler did not operate properly and the sample warmed. The condition was discovered after 76 minutes, irradiation was halted, liquid nitrogen was added, and the infrared spectrum was recorded. Figures 11-13 show the infrared spectra before irradiation, and after 320 and 360 minutes of irradiation had elapsed.

In the second run a 5:1 molar mixture of 3-hexyne: $\text{Fe}(\text{CO})_5$ was used with the cell cooled to 175°K . The results are summarized in Table 4.

Table 3. Results of first run of $\text{Fe}(\text{CO})_5$ and 3-hexyne

Conditions	Observations
77°K Before irradiation	Bands observed at 2106 (w), 1985 (s, br), 1949 (s), and 1684 (w, br)
77°K 5 Min. irradiation	New bands at 2135 (wm) and 1828 (w). Band at 1949 had broadened considerably and extends to $\sim 1956 \text{ cm}^{-1}$
77°K 15 Min. irradiation	Intensity increased at 2135 (wm) cm^{-1}
77°K 45 Min. irradiation	No change
77°K 105 Min. irradiation	Band disappeared at 1684 cm^{-1} . Intensity increased at 2135 (m) and 1828 (m) cm^{-1}
77°K 320 Min. irradiation	Bands observed at 2135 (m), 2106 (w), 2008 (sh), 1985 (s, vbr), 1949-1956 (s, br), 1861 (w) and 1828 (m) cm^{-1} . New band at 1861 (wm) cm^{-1}
77°K 396 Min. irradiation warmed	Bands observed at 2106 (wm), 2055 (s), 2008 (s), 1949 (sh), 1828 (wm), 1800 (w), 1774 (w), 1615 (ms, vbr) and 1516 (w) cm^{-1} . New bands at 2055 (s), 1800 (w), 1774 (w), 1615 (ms, vbr) and 1516 (w) cm^{-1} . Bands disappeared at 2135, 1985, 1861 and 1654 cm^{-1}

Table 4. Results of second run of $\text{Fe}(\text{CO})_5$ and 3-hexyne

Conditions	Observations
175°K, before irradiation	Bands observed at 2020 (sh), 2000 (s), ^a 1947 (ms), 1865 (sh) and 1678 (wm)
175°K, 7 min. irradiation	New bands at 2077 (ms), 2057 (ms), 1972 (s), 1800 (vw), 1773 (vw, br) and 1620 (wm, br). Band disappeared at 1947 cm^{-1} . Intensity decreased at 1678 (wm) cm^{-1}
175°K, 12 min. irradiation	Intensity increased at 1800 (w), 1773 (w) and 1620 (wm, br)
175°K, 20 min. irradiation	New band at 2070 (sh) cm^{-1} . Intensity increased at 1800 (w), 1773 (w) and 1620 (m, br) Intensity decreased at 1678 cm^{-1}
175°K, 30 min. irradiation	Intensity increased at 2070 (sh) cm^{-1} . Intensity decreased at 1678 (vw) cm^{-1}
175°K, 39 min. irradiation	Bands disappeared at 2020 and 1678 cm^{-1} . Intensity increased at 2070 (sh) cm^{-1}
175°K, 51 min. irradiation	Bands observed at 2077 (ms) 2070 (sh), 2057 (sh), 2000 (s), 1972 (s, br), 1865 (sh), 1800 (wm), 1773 (wm), 1703 (vw), 1637 (sh) and 1620 (m)
298°K, after warmup	Bands observed at 2070 (ms), 2000 (s), 1865 (sh), 1773 (m), 1703 (wm), 1637 (m) and 1620 (m) cm^{-1}

^aChart paper was moved so that it corresponded with the instrument reading.

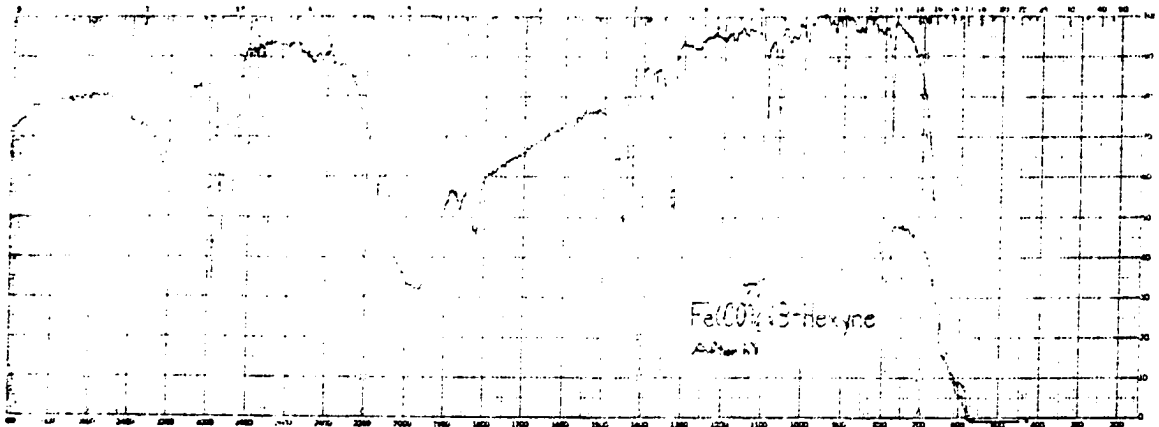


Figure 12. First run of $\text{Fe}(\text{CO})_5 + 3\text{-hexyne}$ at 77°K after irradiation for 320 min.

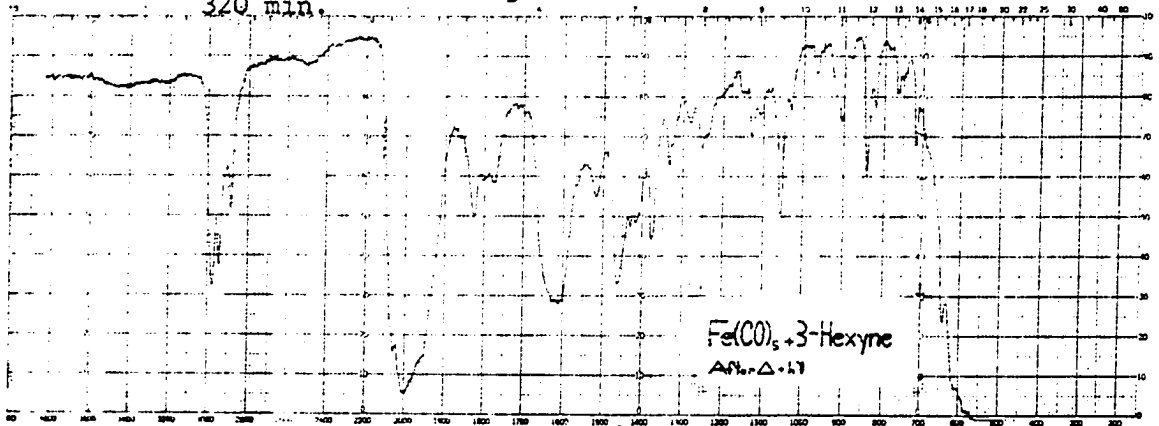


Figure 13. First run of $\text{Fe}(\text{CO})_5 + 3\text{-hexyne}$ at 77°K after warming and irradiation for 396 min.

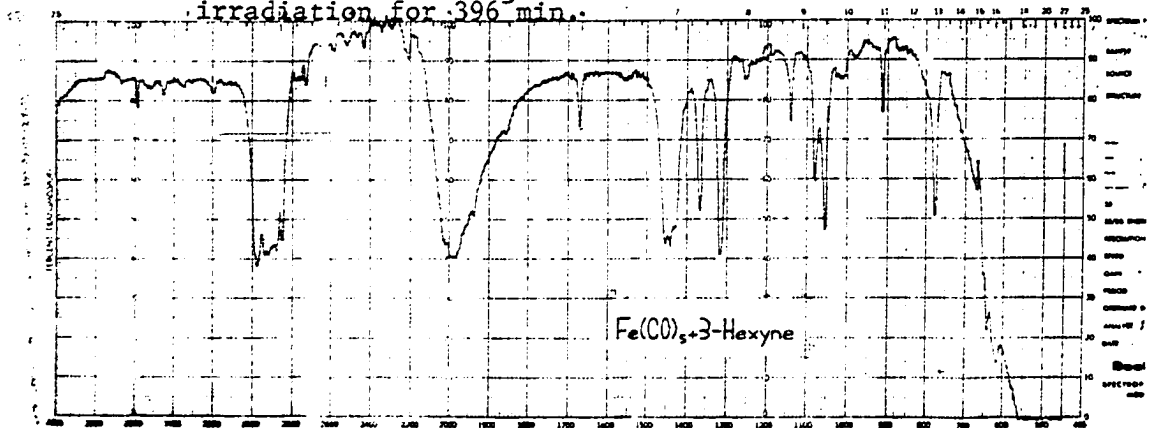


Figure 14. Second run of $\text{Fe}(\text{CO})_5 + 3\text{-hexyne}$ at 171°K before irradiation

Figures 14, 15 and 16 show the infrared spectra before irradiation, after irradiation and after warmup, respectively. More detailed traces of the 2100-1950, 1750-1850, and 1600-1700 cm^{-1} regions during irradiation are shown in Figures 17-19, while Figures 20 and 21 show the 2080-2040 and 1680-1850 cm^{-1} regions during warmup.

In the third run a 5:1 3-hexyne: $\text{Fe}(\text{CO})_5$ molar mixture was again used. It had been noticed that a red-orange precipitate formed on mixing the reagents in the dark. Therefore, the mixture was first centrifuged and the liquid layer then was transferred to salt plates. All attempts to isolate the precipitate led to polymeric material containing no metal complexed- or organic-carbonyl infrared bands. The results of the run utilizing the liquid layer are summarized in Table 5.

Table 5. Results of third run of $\text{Fe}(\text{CO})_5$ + 3-hexyne

Conditions	Observations
77°K, before irradiation	Bands observed at 2039 (m), 1995 (sh), 1980 (s), 1969 (s), 1955 (m), 1948 (m), 1680 (w) and 1575 (w) cm^{-1}
77°K, 5 min. irradiation	No change
77°K, 20 min. irradiation	No change
77°K, 252 min. irradiation	New bands at 1815 (wm) and 1822 (wm) cm^{-1} . Band disappeared at 1680 cm^{-1}
77°K, 629 min. irradiation	Bands observed at 2039 (m), 1995 (sh), 1980 (s), 1969 (s), 1955 (sh), 1948 (sh) and 1818 (w, br) cm^{-1}
77°K, after warmup	Bands observed at 2060 (sh), 2025 (m), 1998 (ms), 1990 (sh) and 1818 (m)

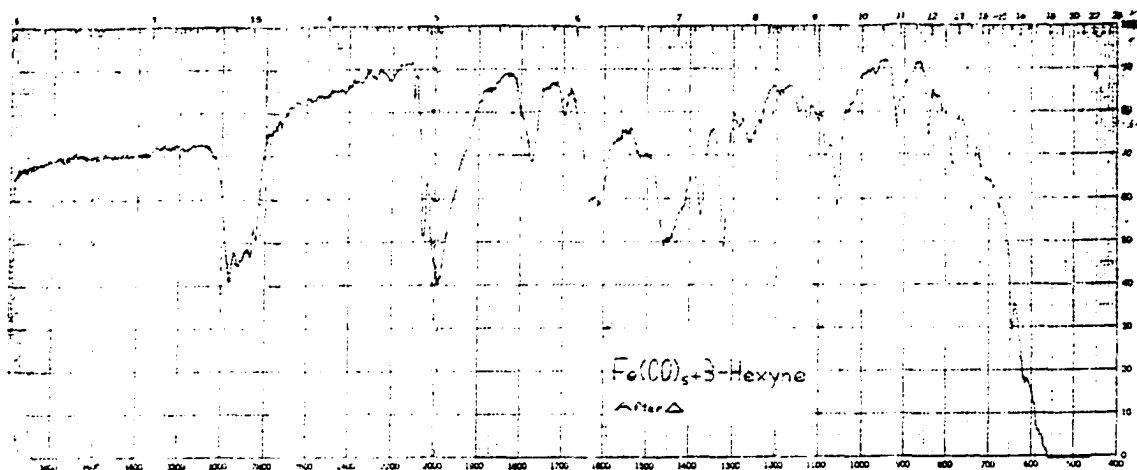


Figure 15. Second run of $\text{Fe}(\text{CO})_5 + 3\text{-hexyne}$ at 296°K after warmup

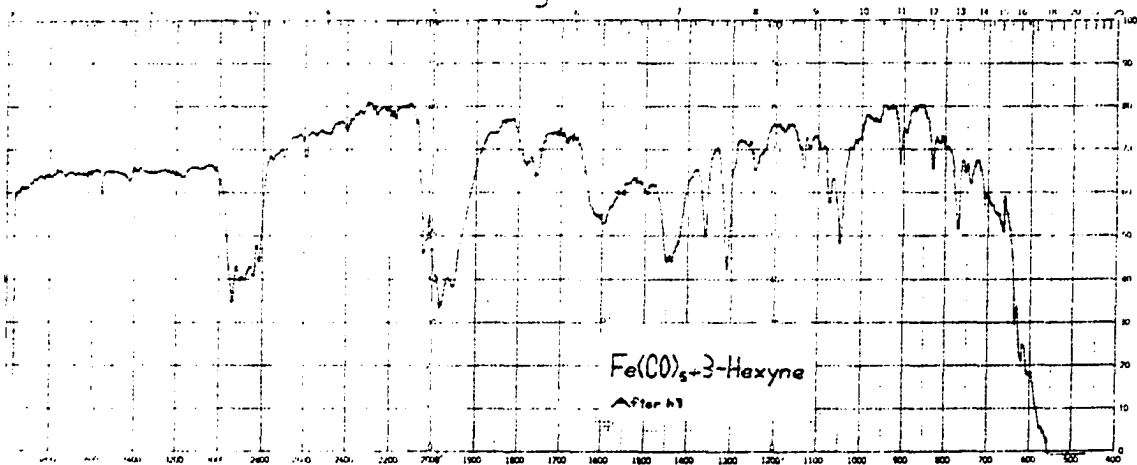


Figure 16. Second run of $\text{Fe}(\text{CO})_5 + 3\text{-hexyne}$ at 171°K after irradiation

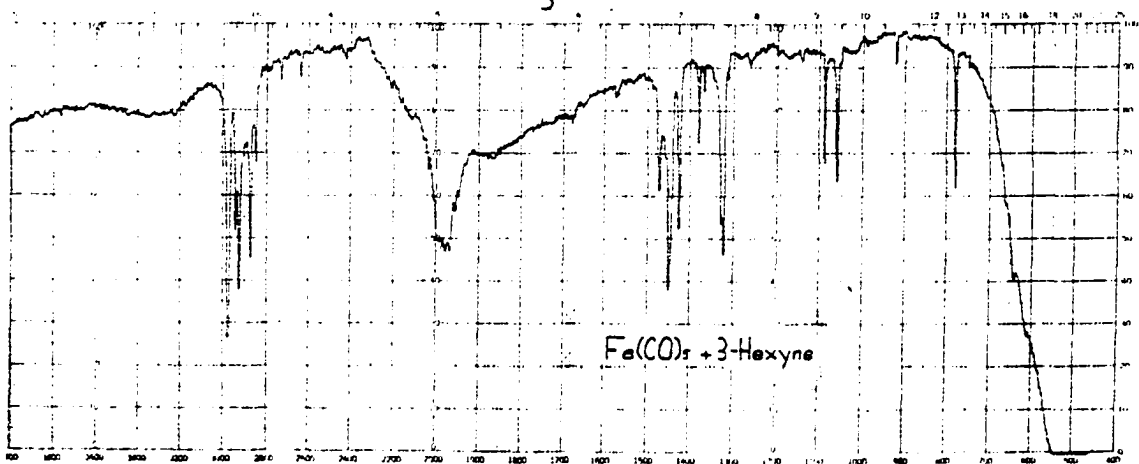


Figure 17. Third run of $\text{Fe}(\text{CO})_5 + 3\text{-hexyne}$ at 77°K before irradiation

Figure 18. Second run of $\text{Fe}(\text{CO})_5 + 3\text{-hexyne}$; 2100-1950 cm^{-1} region during irradiation, a = 7 min.,
b = 12 min., c = 20 min., d = 30 min., e = 39 min.

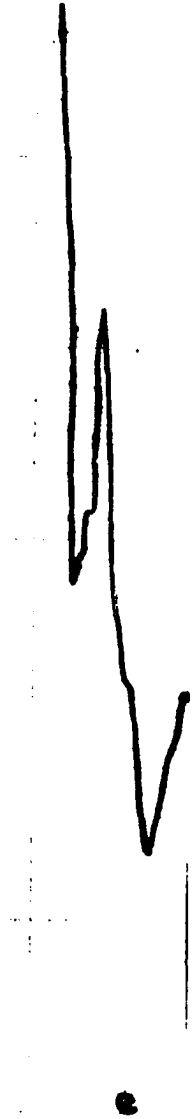
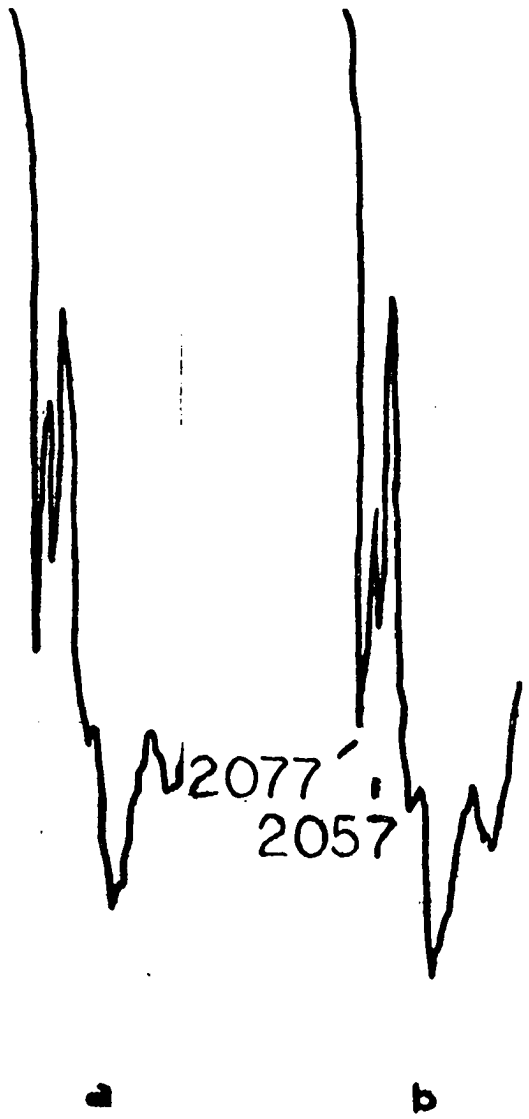
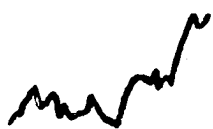


Figure 19. Second run of $\text{Fe}(\text{CO})_5 + 3\text{-hexyne}$; $1850\text{-}1750\text{ cm}^{-1}$ region during irradiation;
a = 7 min., b = 12 min., c = 20 min., d = 30 min., e = 39 min.



a



b



1800 1773

c



d



e

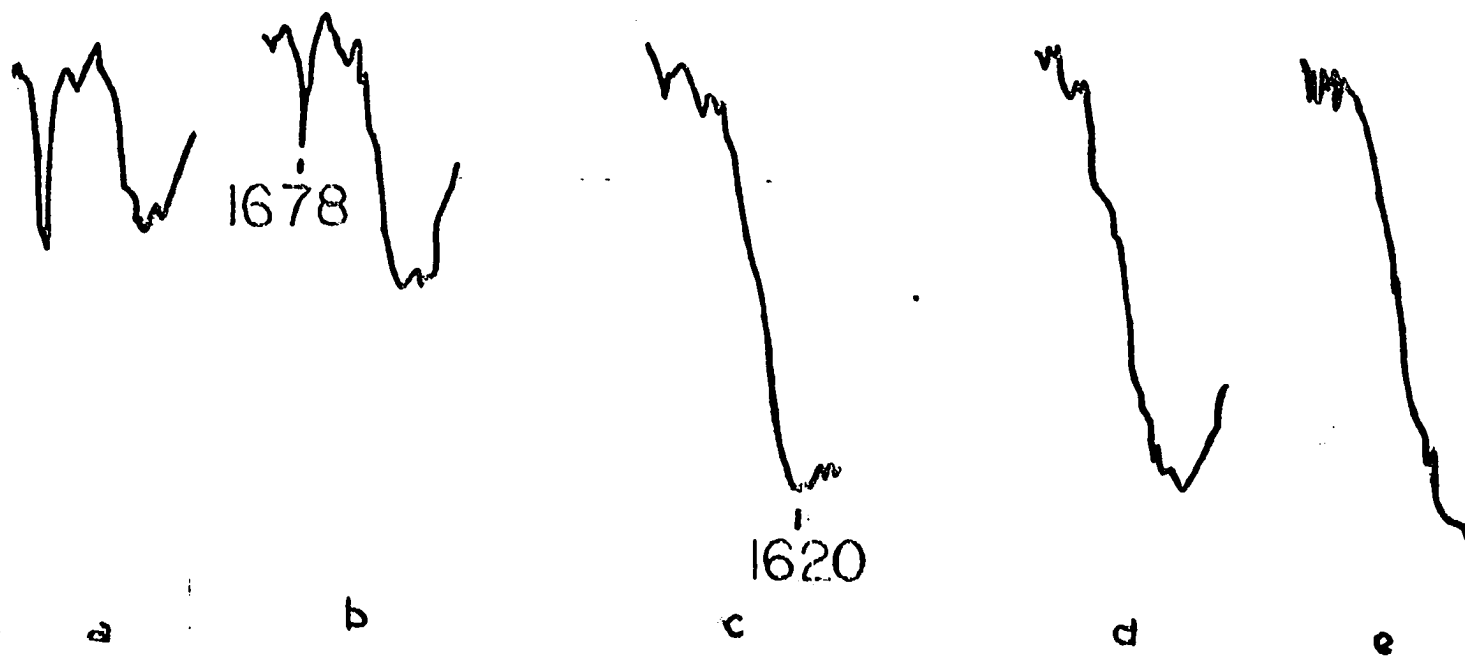


Figure 20. Second run of Fe(CO)₅ + 3-hexyne; 1700-1600 cm⁻¹ region during irradiation; a = 7 min., b = 12 min.; c = 20 min; d = 30 min.; e = 39 min.

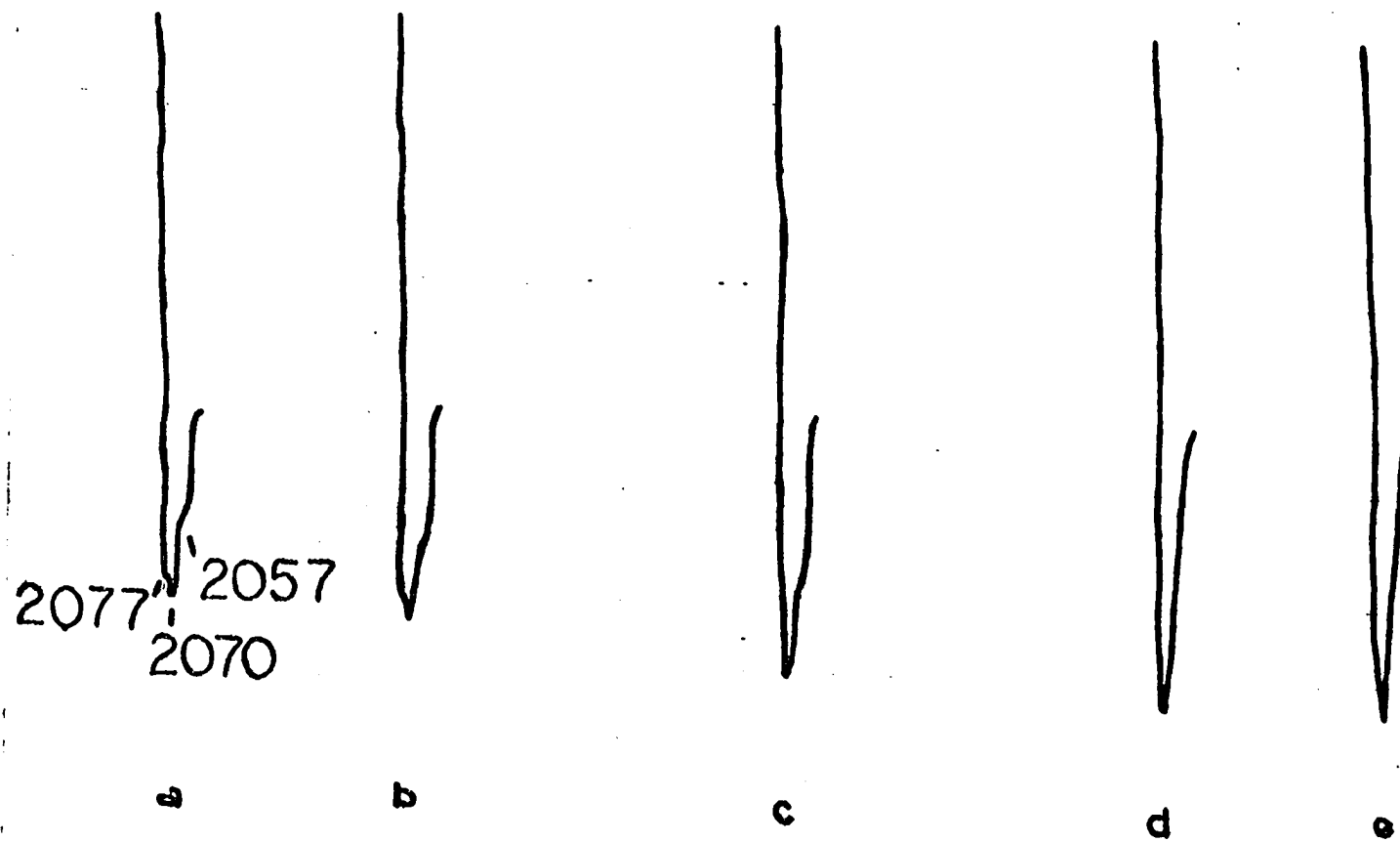
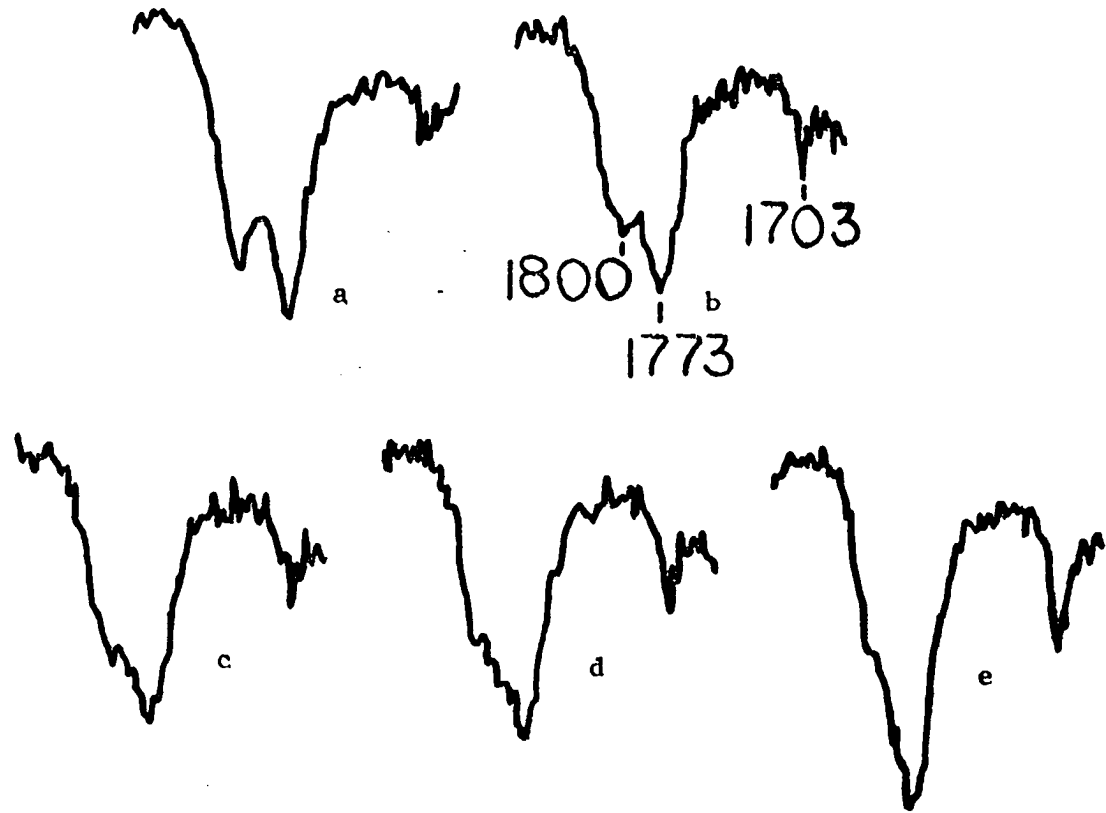


Figure 21. Second run of $\text{Fe}(\text{CO})_5 + 3\text{-hexyne}$; 2080-2040 cm^{-1} region during warmup; a = 171 $^\circ\text{K}$;
 b = 195 $^\circ\text{K}$; c = 232 $^\circ\text{K}$; d = 252 $^\circ\text{K}$; e = 260 $^\circ\text{K}$

Figure 22. Second run of $\text{Fe}(\text{CO})_5$ + 3-hexyne; 1850-1680 cm^{-1} region during warmup; a = 171^oK,
b = 243^oK, c = 252^oK, d = 260^o, e = 284^oK



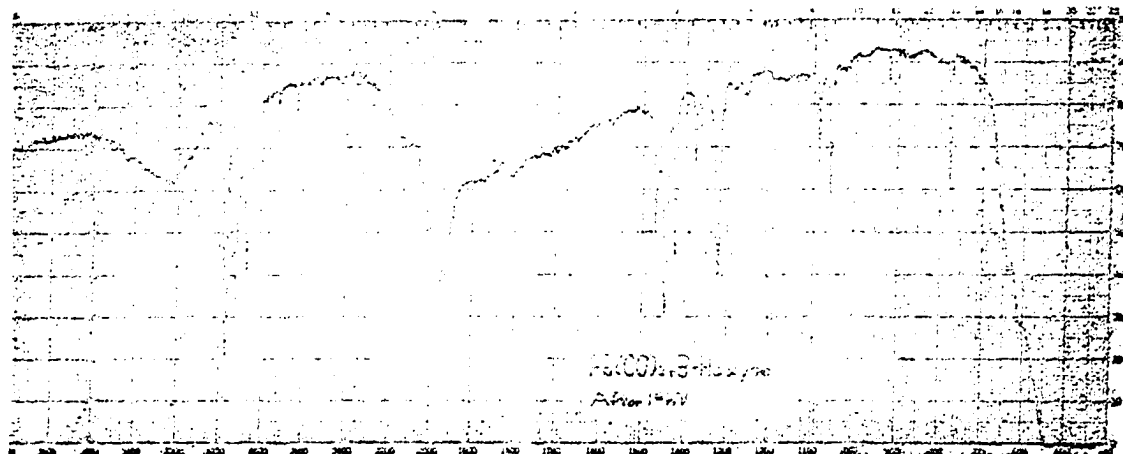


Figure 23. Third run of $\text{Fe}(\text{CO})_5 + 3\text{-hexyne}$ at 77°K after irradiating for 629 min.

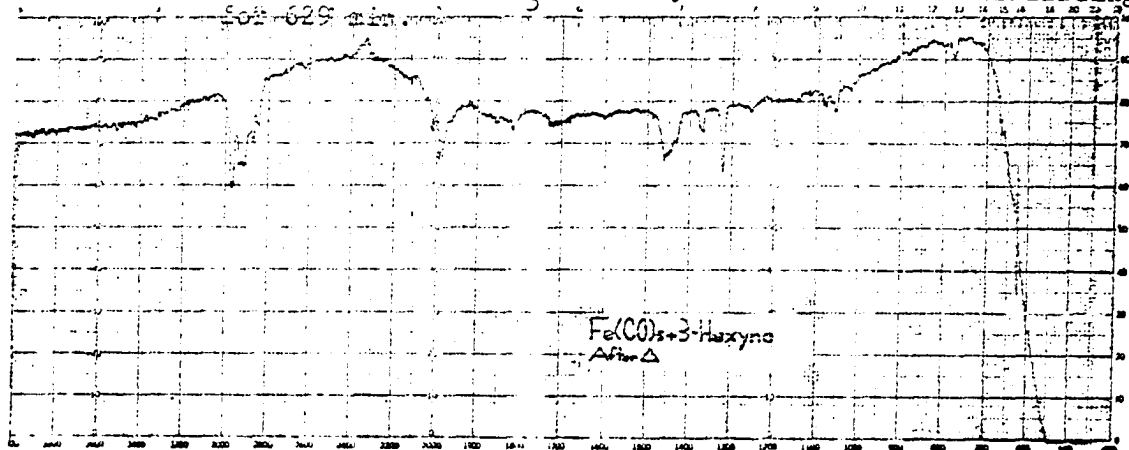


Figure 24. Third run of $\text{Fe}(\text{CO})_5 + 3\text{-hexyne}$ after warmup

The experiments involving diethylacetylene and $\text{Fe}(\text{CO})_5$ introduce many complexities. First, we are dealing with two component photochemical reactions rather than unimolecular reactions. Second, various thermal, dark reactions occur before the reactants are cooled. Third, the various thermal and photochemical products have a chemistry of their own which further clouds the interpretation. However, some success has been obtained in explaining the results.

Diethylacetylene has been shown (56) to be unreactive photochemically under the reaction conditions. The chemistry of $\text{Fe}(\text{CO})_5$ is evident, however, in the results. In the first run, the 1956 cm^{-1} band is attributable to $\text{Fe}(\text{CO})_4$, and the band at 2135 cm^{-1} is associated with CO probably arising from photodissociation of $\text{Fe}(\text{CO})_5$ or perhaps from an organoiron carbonyl intermediate.

In the second run much of the $\text{Fe}(\text{CO})_5$ has reacted with 3-hexyne before cooling and the 1947 cm^{-1} band, which can be assigned to an intermediate or $\text{Fe}(\text{CO})_5$, quickly disappears upon irradiation. It is noteworthy that no evidence for $\text{Fe}_2(\text{CO})_9$ in the 1820 cm^{-1} region is observed. In the third run some $\text{Fe}_2(\text{CO})_9$ formation is observed with the bands at 1815, 1818 and 1822 cm^{-1} .

The variations in $\text{Fe}_2(\text{CO})_9$ formation in the three runs is of interest. The dark reaction especially in runs 2 and 3 depletes the amount of $\text{Fe}(\text{CO})_5$ present before irradiation, thus the observation of little or no $\text{Fe}_2(\text{CO})_9$ observed in the last two runs. Evidently, the reaction product of the initial interaction of $\text{Fe}(\text{CO})_5$ and 3-hexyne is more reactive toward 3-hexyne than is $\text{Fe}(\text{CO})_5$. A more detailed discussion of the overall mechanism will be given below. Therefore, in the first run

where the 3-hexyne:Fe(CO)₅ molar ratio is only 2:1, some Fe(CO)₅ remains and reacts through Fe(CO)₄ to form Fe₂(CO)₉. The formation of Fe₂(CO)₉ occurs at lower temperature in the matrix formed in runs 1 and 3 than in the matrix of Fe(CO)₅ discussed in the previous section. Why Fe(CO)₄ is more stable in the latter environment is not clear.

With some understanding of the behavior of the starting reactants, the formation of quinones as well as other products can be explored. As previously described, the principle products of the photochemical reaction of Fe(CO)₅ with 3-hexyne (38) are tetraethylbenzoquinone-tricarbonyliron (9a) and tetraethylbenzoquinone (7b). 9a has ir bands (38) at 2066, 2012, 1639 and 1618 cm⁻¹, and 7b has a band (57) at 1634 cm⁻¹.

In runs 1 and 3 the compound, A, with a band at ~1680 cm⁻¹ was present in only very small quantity. The absence of A in the third run is attributed to the centrifuging of the reaction mixture prior to cooling. The red-orange precipitate must have had the 1680 cm⁻¹ band observed in run 2, since centrifuging was the only difference in sample preparation. In the first run, however, the formation of only a very small amount of A must involve the change in relative concentration of the starting materials. In run 1, the molar ratio of 3-hexyne:iron pentacarbonyl was 2:1, while in runs 2 and 3, the ratio was 5:1. Evidently, a high 3-hexyne:iron pentacarbonyl ratio is needed for formation of A.

Upon irradiation the ~1680 cm⁻¹ band decreases and then disappears. In runs 1 and 3, the concentration of A is small and no changes in the infrared spectrum are noticed as the ~1680 cm⁻¹ band disappears.

However, in run 2 dramatic changes occur. As the 1678 cm^{-1} band disappears, new bands are observed at 2077, 2070, 2057, 1800, 1773, 1637 and 1620 cm^{-1} . None of these bands were observed during low temperature irradiation in runs 1 and 3. It can, therefore, be concluded that A is a necessary precursor for further reaction.

The results of run 1 are somewhat anomalous in the context of the above conclusions. Although the 1684 cm^{-1} band is initially very weak, and disappears upon irradiation to yield no observable bands, bands at 1800, 1774 and 1615 cm^{-1} are observed when irradiation and warmup occur simultaneously.

If A is necessary for new compound formation, then conditions must have changed in the initial irradiation period to allow formation of A during the warmup stage. The newly formed A then reacts under the photolytic conditions to produce the observed bands of the new compounds. In run 1, the chief process which is observed during irradiation is the production of $\text{Fe}_2(\text{CO})_9$. The resulting decrease in $\text{Fe}(\text{CO})_5$ must allow the later formation of A. Thus, the high concentration of $\text{Fe}(\text{CO})_5$ may be inhibiting compound formation either by promoting an alternate pathway or by influencing a step prior to product formation. This influence could involve a different concentration effect. The depletion of $\text{Fe}(\text{CO})_5$ leads to an increase in 3-hexyne relative concentration which would allow the process leading to the formation of A to proceed during warmup.

Compound B, represented by the 1800 cm^{-1} band can either contain a bridged polynuclear iron carbonyl or a strained organic carbonyl moiety. In run 2, as warmup occurs, the 1800 cm^{-1} band disappears with the

concomitant formation of compound C which is probably an organic-carbonyl compound with a band at 1703 cm^{-1} . For run 1, in contrast, conditions did not lead to further reaction of B. Perhaps the temperature was not high enough to provide the activation energy for formation of C. The nature of B and C are unknown, but could involve the rearrangement of tetraethylbicyclopentadieneone to tetraethylcyclopentadieneone. An alternate explanation could be the unavailability of additional $\text{EtC}\equiv\text{CEt}$ in run 1 needed for B to react during warmup.

The bands at 1637 and 1620 cm^{-1} in run 2 and at 1615 (vbr) cm^{-1} in run 1 are attributed to 9a. In run 2, 9a is formed upon irradiation and occurs with the disappearance of A. In run 1, the absence of A before irradiation leads to the absence of 9a during irradiation of the sample. However, during photolysis and warmup 9a is formed. Again a reasonable explanation involves the formation of A during warmup and subsequent photolysis to form 9a. In run 3, the absence of A again results in no formation of 9a during irradiation. Whether the free tetraethylbenzoquinone (7b) is also present is not known with certainty, but could be present from the loss of $(\text{Fe}(\text{CO})_3)$ from 9a during irradiation.

The band at 1773 cm^{-1} is assigned to compound D of unknown structure. It has a similar history of formation at B and 9a and survives irradiation, warmup, and irradiation during warmup.

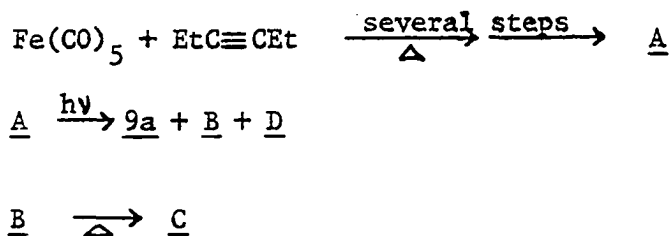
The bands at 2055 cm^{-1} in run 1, and 2077 and 2057 cm^{-1} in run 2 will now be discussed. In run 2, these bands appear after 7 minutes and remain almost unchanged during the course of the irradiation. During warmup both bands disappear. They appear before the 1678 cm^{-1} band has lost very much intensity and it is not clear whether A is a necessary precursor. However, since neither the 2077 nor the 2057 cm^{-1}

band are observed in run 3 it would appear that A is needed. In run 1, the 2055 cm^{-1} band occurs on warmup during photolysis. The observation of a doublet in the second run as opposed to the single band in run 1 may be caused by the different conditions used to record the spectra. The bands at 2077 and 2057 cm^{-1} behave similarly to the 1800 cm^{-1} band and probably are also associated with B.

The band at 2070 cm^{-1} could be assigned to 9a. However, the absence in run 1 is difficult to understand, and further investigation will be necessary to identify this band. Also unexplained is the loss of bands in the $1950\text{-}1920\text{ cm}^{-1}$ region in run 3 during warmup.

A comparison of Hübel's proposed scheme (51) in relation to the results described above is of interest. As previously described the scheme involves the intermediacy of complexes of the type $\text{RC}_2\text{RFe}(\text{CO})_4$ (13) and $\text{RC}_2\text{RFe}_2(\text{CO})_7$ (15). For $\text{R} = \text{Et}$, neither complex has been isolated and the involvement of 13 and 15 is inferred by the formation of analogous compounds from bulky alkyls or aromatic acetylenes. Since neither 13 nor 15 have any bridging or organic carbonyl groups, their detection within a reaction mixture is quite difficult. However, the observation of B, C and D in various stages of the reaction is not explained by the details of the scheme and indeed by any product previously described for the acetylene-iron carbonyl reactions. Also, the observation that A is necessary for quinone formation was not observed by Hübel and his coworkers. Thus, while the framework of the scheme may be correct, additional intermediates and products seem to be involved. In the absence of structural information of compounds A - D, no alternate scheme will be proposed. However, summary of the results

follow:



Iron Pentacarbonyl and Diphenylacetylene

A 5:1 molar ratio of diphenylacetylene:iron pentacarbonyl in diethyl ether was cooled to 77°K. The infrared spectrum of the resulting white glass is shown in Figure 25. Major bands were observed at 2004 (sh), 1993 (sh), 1987 (s), 1955 (sh), and 1603 (m). After irradiating for 490 minutes, the infrared spectrum, Figure 26, of the gray-green material showed new bands at 2138 (m), 1825 (ms), and 1818 (ms) cm⁻¹. The 1950-2060 cm⁻¹ region was a single, broad band. The material was warmed to 214°K and quickly cooled to 77°K. The infrared spectrum in Figure 27 of the green material showed the disappearance of the 2138 cm⁻¹ band and the increase in the new coalesced band at 1822 (ms) cm⁻¹.

In the second run, a 1:2 diphenylacetylene:iron pentacarbonyl molar mixture was cooled to 190°K. A summary of the results appears in Table 6.

Table 6. Results of second run of diphenylacetylene and iron pentacarbonyl

Conditions	Observations
173°K, before irradiation	Bands observed at 2018 (s), 1994 (s), 1958 (ms), 1952 (ms), 1885 (ms), 1833 (m), 1762 (m), 1677 (m), and 1604 (ms) cm^{-1}
173°K, 5 min. irradiation	New bands at 2092 (m) and 1940 (ms) cm^{-1}
173°K, 10 min. irradiation	Intensity increased at 2092 (m) cm^{-1}
190°K, 25 min. irradiation	New bands at 2081 (m) and 1817 (sh) cm^{-1}
190°K, 105 min. irradiation	Bands observed at 2092 (m), 2081 (m), 2018 (s), 1994 (s), 1952 (ms), 1940 (sh), 1885 (ms), 1833 (m), 1817 (m), 1762 (m), 1677 (wm) and 1604 (ms) cm^{-1}
298°K, after warmup	Bands observed at 2081 (w), 2035 (vs), 2018 (vs), 1985 (sh, br), 1952 (wm), 1885 (wm), 1825 (wm, vbr), 1743 (ms), 1737 (ms), 1677 (vs), and 1604 (wm)

Figures 28-30 show the complete ir spectra before irradiation, after irradiation, and following warmup. Details of the changes in the 2100-1900 cm^{-1} region during irradiation and warmup are seen in Figures 31-32.

These experiments were undertaken in an effort to unravel the very complex reactions between iron pentacarbonyl and diphenylacetylene. Under the conditions employed, some of the results obtained were novel and unexpected.

In the first run, the use of a high diphenylacetylene:iron pentacarbonyl ratio led to the lack of product formation in the dark. This result is in sharp contrast to the observations involving 3-hexyne and $\text{Fe}(\text{CO})_5$ where extensive dark reactions occurred. Evidently the

Figure 25. First run of $\text{Fe}(\text{CO})_5$ + diphenylacetylene at 77°K before irradiation

Figure 26. First run of $\text{Fe}(\text{CO})_5$ + diphenylacetylene at 77°K after irradiation

Figure 27. First run of $\text{Fe}(\text{CO})_5$ + diphenylacetylene at 77°K following warmup

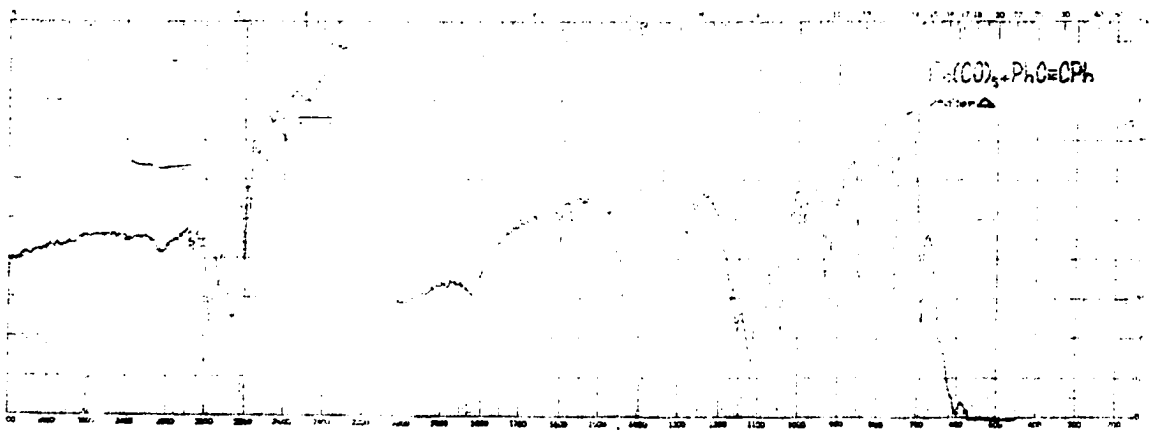
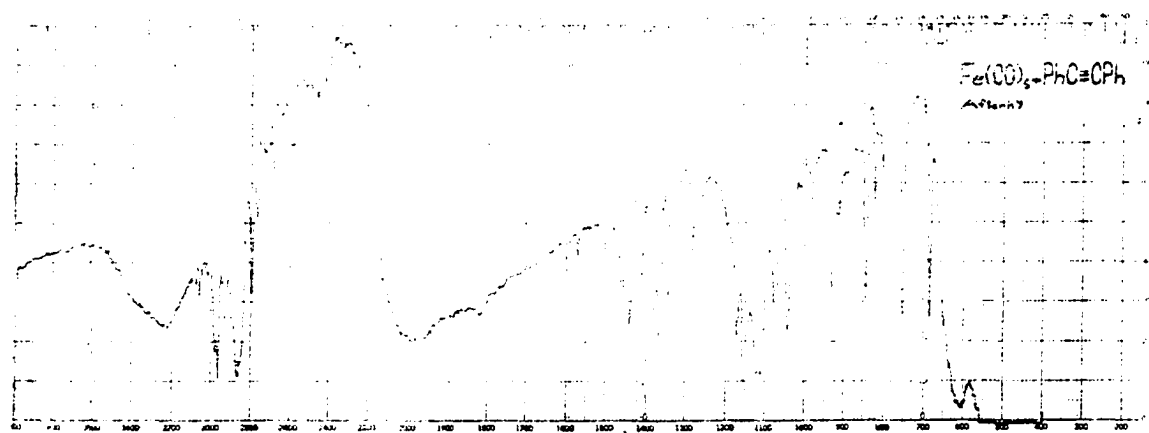
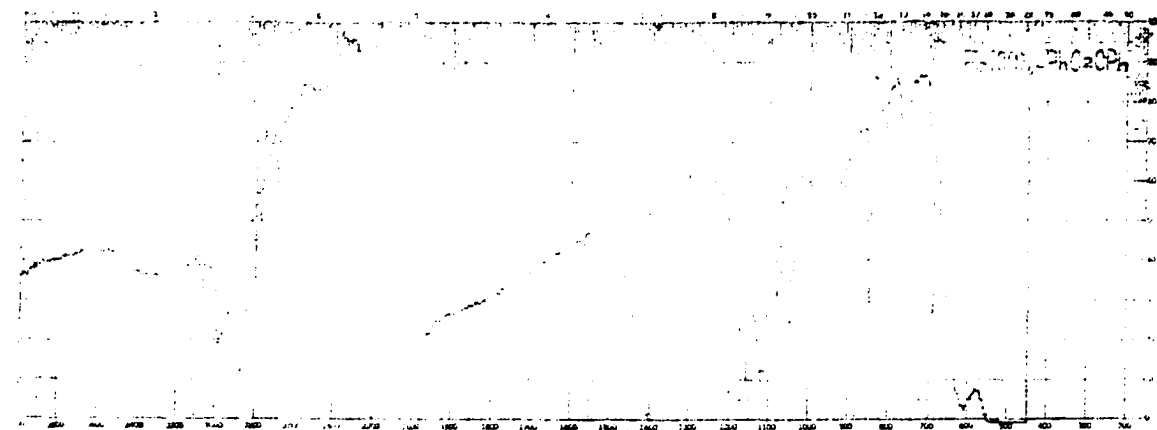


Figure 28. Second run of $\text{Fe}(\text{CO})_5$ + diphenylacetylene at 173°K before irradiation

Figure 29. Second run of $\text{Fe}(\text{CO})_5$ + diphenylacetylene at 190°K after irradiation for 105 min.

Figure 30. Second run of $\text{Fe}(\text{CO})_5$ + diphenylacetylene at 298°K after warmup

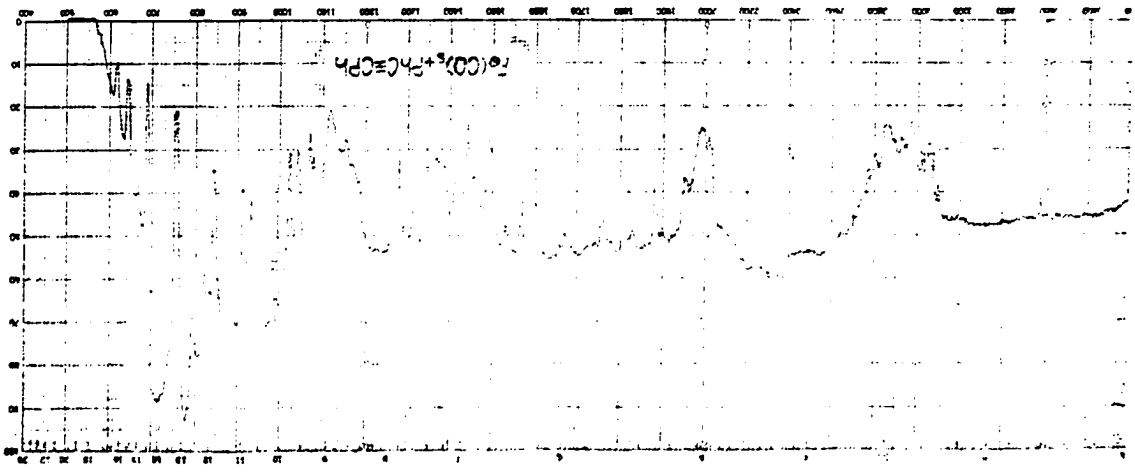
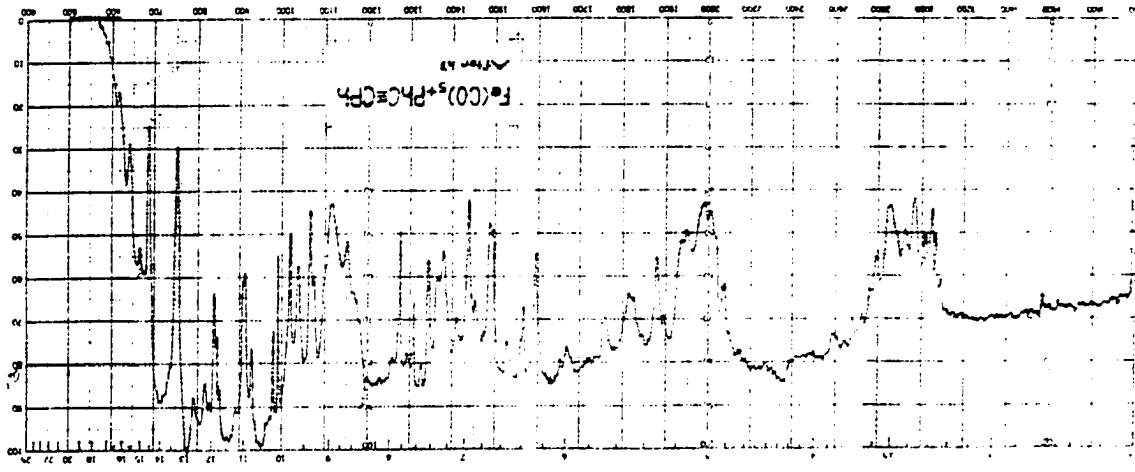
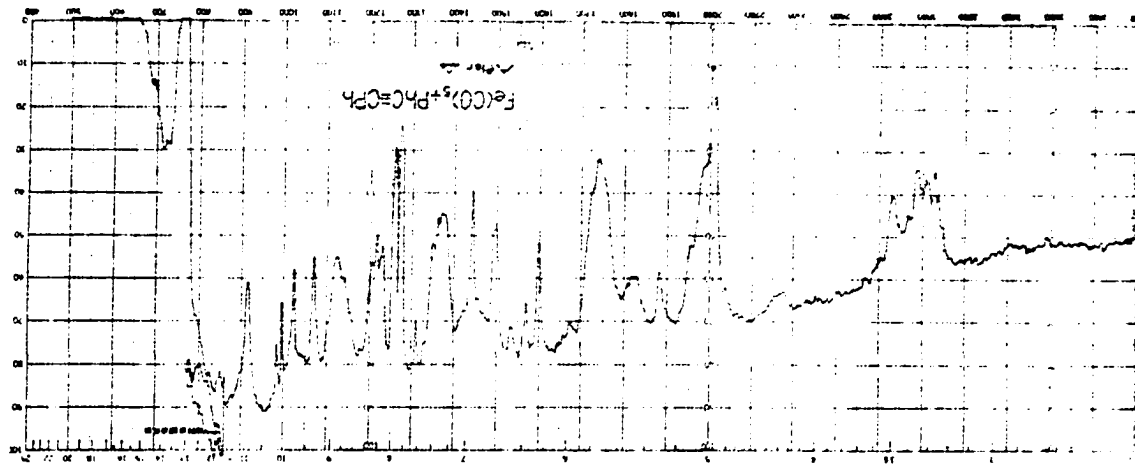
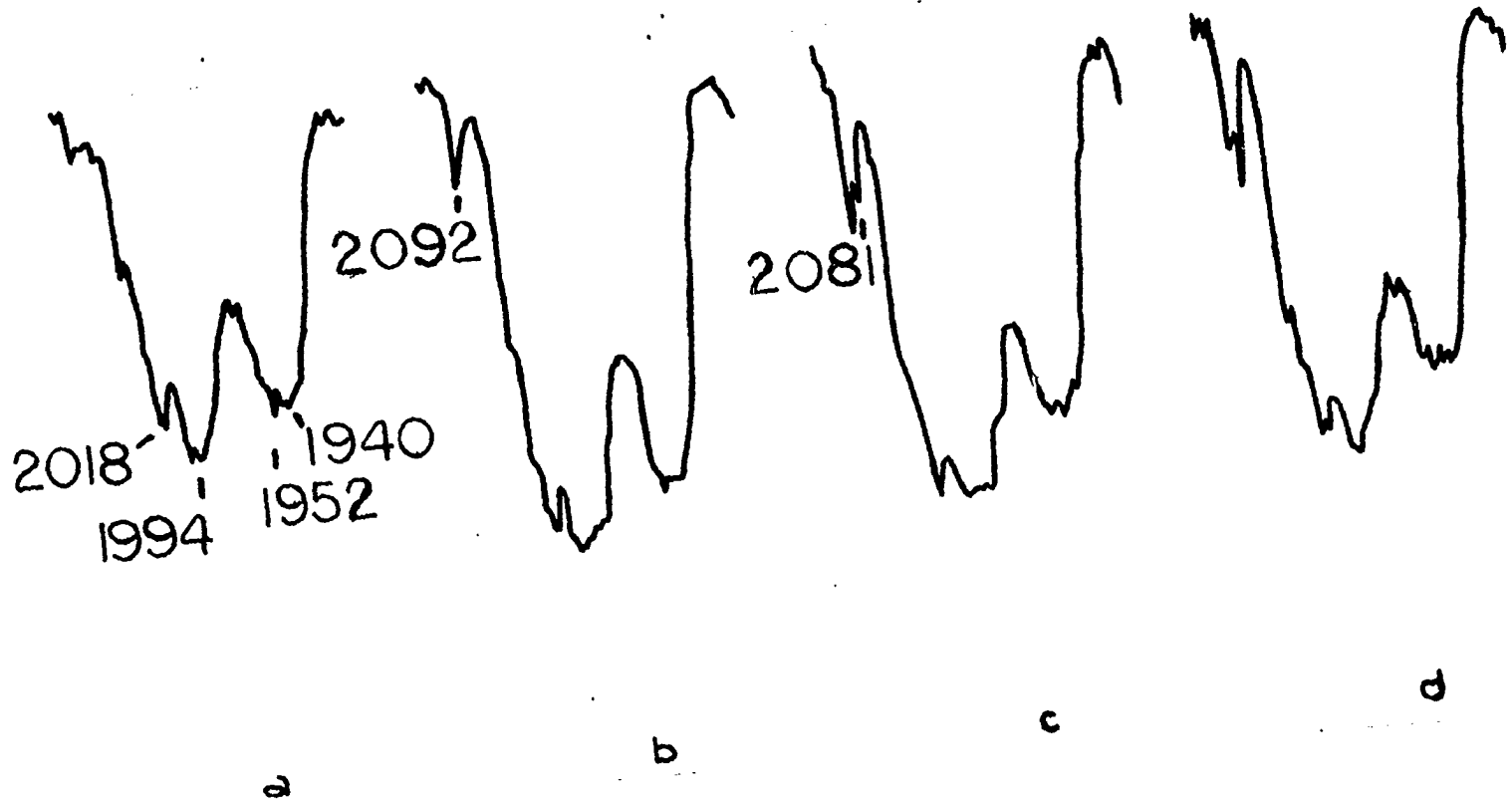


Figure 31. Second run of $\text{Fe}(\text{CO})_5$ + diphenylacetylene during irradiation, 2100-1900 cm^{-1} region;
a = 5 min., b = 10 min., c = 25 min., d = 35 min., e = 45 min., f = 60 min., g = 75 min.
(shown on p. 49a-49b)



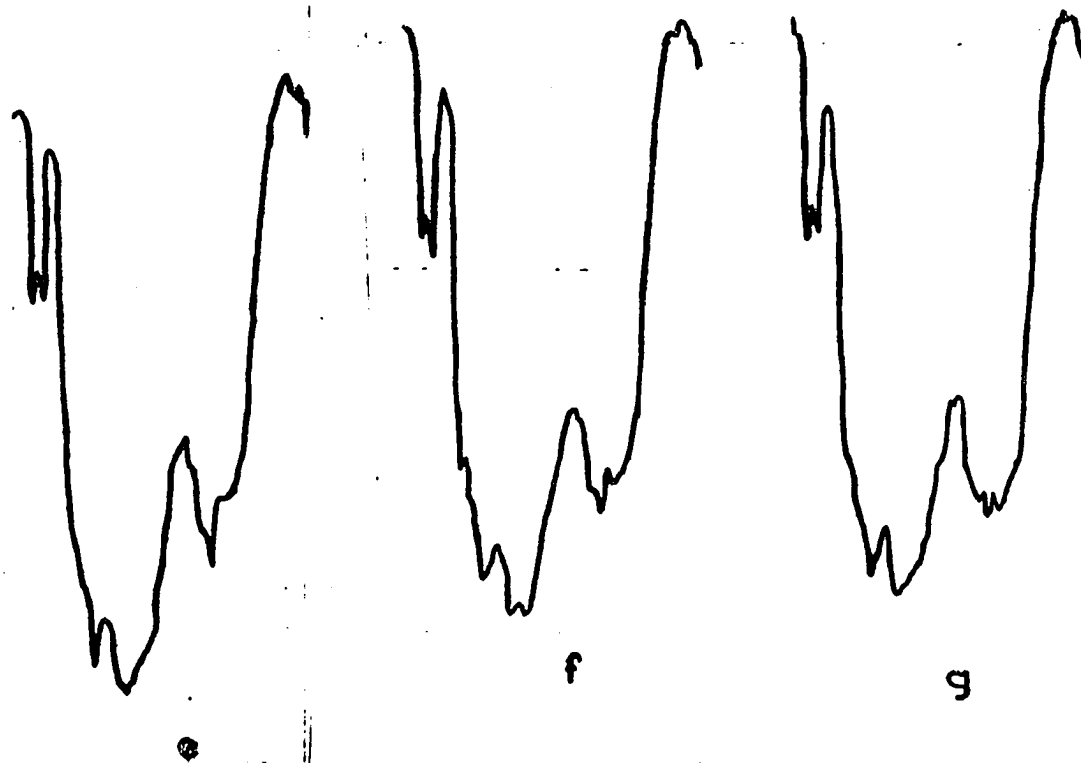
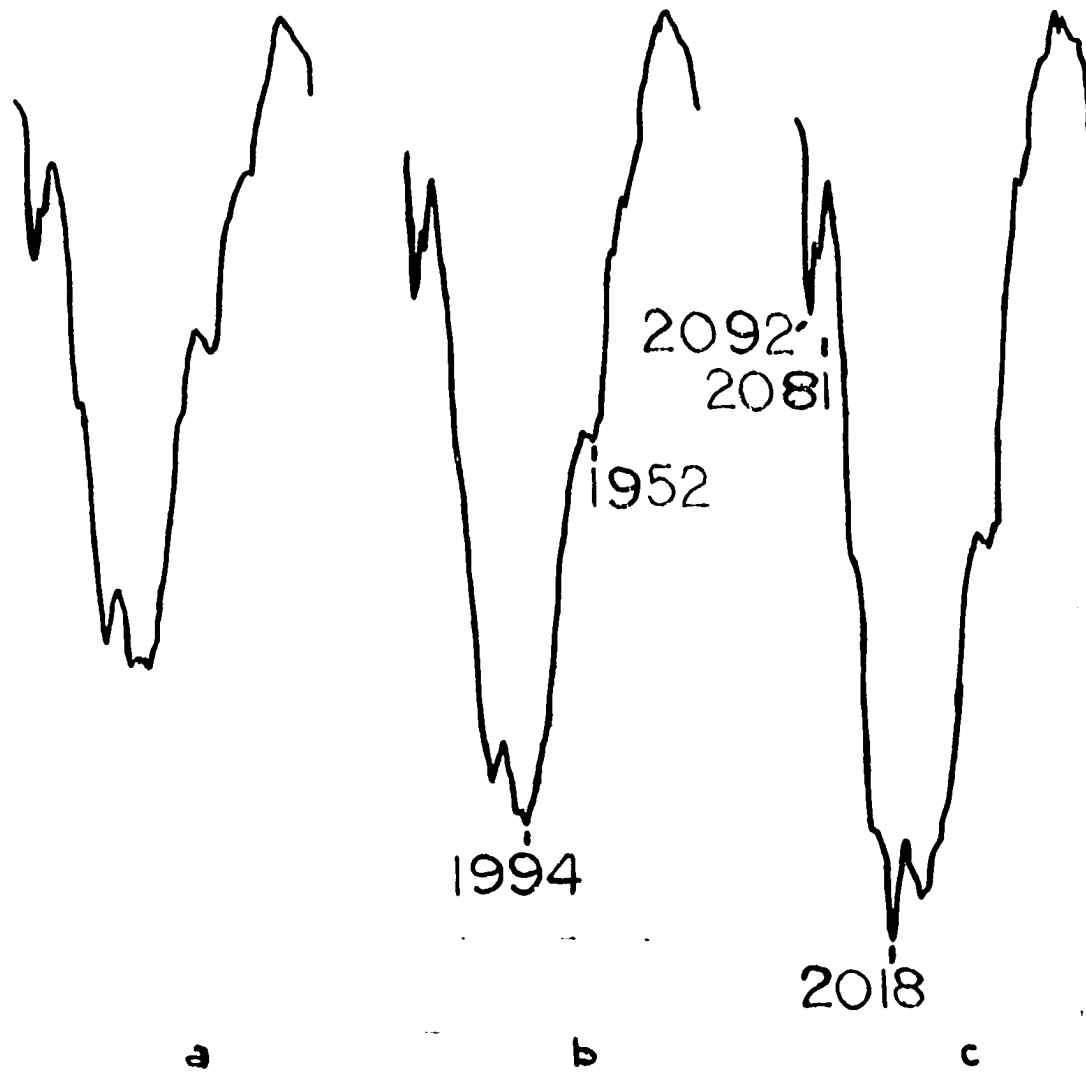


Figure 31 continued

Figure 32. Second run of $\text{Fe}(\text{CO})_5 + 3\text{-hexyne}$; $2100\text{-}1900\text{ cm}^{-1}$ region during warmup, a = 209°K ,
b = 226°K , c = 238°K , d = 249°K , e = 258°K
(shown on p. 51a-51b)



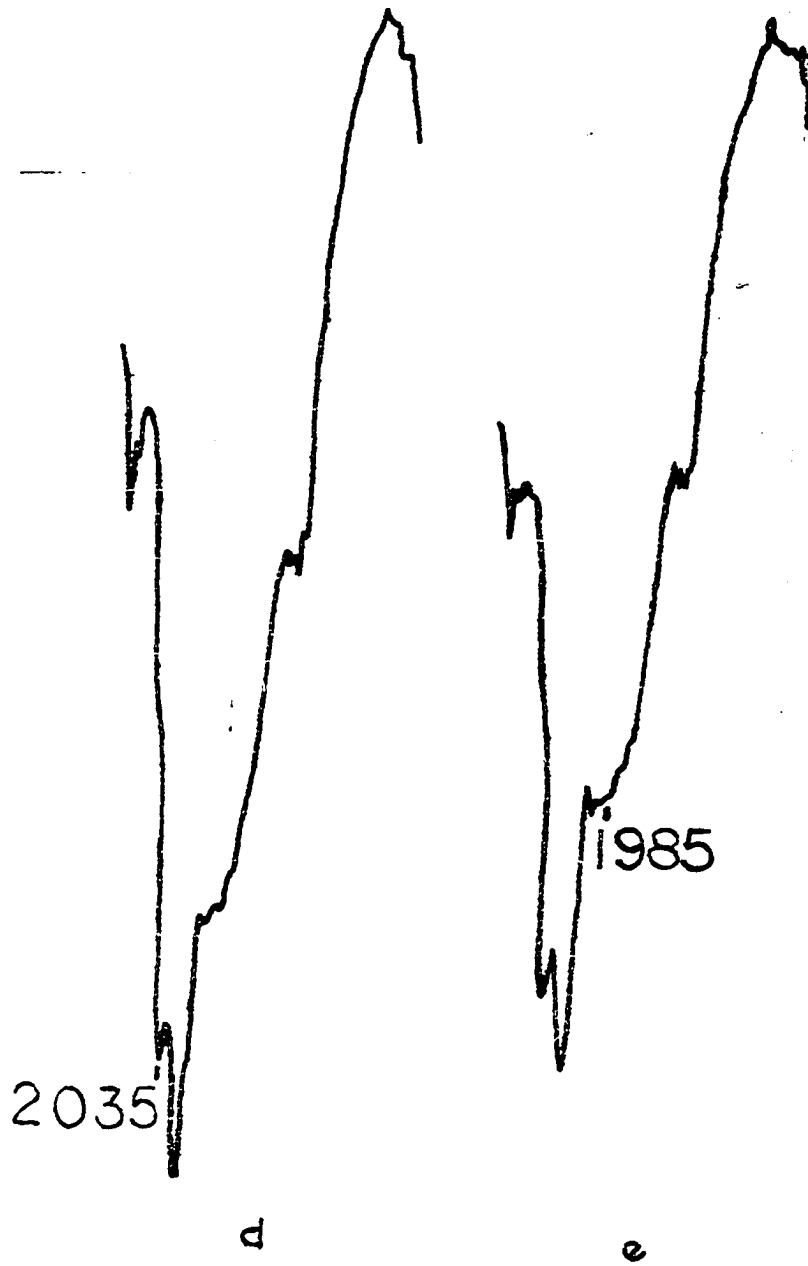


Figure 32 continued

Table 7. Products of the interaction of diphenylacetylene and various iron carbonyls

Compound	Carbonyl infrared bands (cm^{-1})	Reference
<u>11a</u>	2033, 1965, 1931	40
<u>2b</u>	2062, 2012, 1988, 1642	40
<u>12a</u>	2062, 2024, 1980, 1923	40
<u>3a</u>	2075, 2024, 1992, 1976, 1927	40
<u>5a</u>	2075, 2053, 2016, 1667	40
<u>4a</u>	2066, 2012, 1976, 1852	40
<u>16a</u>	2130, 2060, 2030, 1660	52

nature of the acetylene substituent plays an important role in determining the course of the reaction. The use of diethyl ether solvent may also have contributed to the change in reactivity.

Upon irradiation at 77°K a now well established process occurs. Free CO is observed and $\text{Fe}(\text{CO})_4$ diffuses through the matrix to form $\text{Fe}_2(\text{CO})_9$. On warmup, the free CO escapes and the $\text{Fe}_2(\text{CO})_9$ bands at 1818 and 1825 cm^{-1} increase.

In the second run a change in the molar ratio of the starting materials led to product formation at room temperature in the dark. Again $\text{Fe}(\text{CO})_9$ is a product. The bands at 1833 and 1817 cm^{-1} are assigned to $\text{Fe}_2(\text{CO})_9$ and increase during the period of irradiation. During warmup a single broad band at $\sim 1825\text{ cm}^{-1}$ is formed.

Probably the most surprising result of this experiment is that no previously identified organoiron compound is formed. In Table 7 are listed relevant products of the interaction of diphenylacetylene and any of the iron carbonyls. As can be seen, none of the listed bridging or organic carbonyl bands correspond to those observed in run 2.

Of the starting bands, the 1604 cm^{-1} band arises from the phenyl groups present, and the 2018 , 1994 and 1952 cm^{-1} bands are attributable to CO stretching in $\text{Fe}(\text{CO})_5$ or in organoiron carbonyl compound. The 1885 cm^{-1} band also is assigned to a complexed iron carbonyl CO stretch since a metal bridging CO normally arises in the $1800\text{--}1850\text{ cm}^{-1}$ region, and except for cyclopropeneones organic carbonyls do not occur in the 1885 cm^{-1} region. The possibility that a cyclopropeneone is not involved cannot be completely ruled out although such a compound has never been isolated in reactions involving the starting materials. A more probable assignment is either $(\text{PhC}_2\text{Ph})\text{Fe}(\text{CO})_4$ or $(\text{PhC}_2\text{Ph})\text{Fe}_2(\text{CO})_7$ described by Hübel (58). As previously described the 1833 cm^{-1} band is associated with $\text{Fe}_2(\text{CO})_9$. The remaining bands at 1762 and 1677 cm^{-1} are most probably associated with organic ketones of unknown structure.

Little change occurs to the initial bands upon irradiation. The band at 1677 cm^{-1} decreases somewhat intensity while, as described above, that at 1833 cm^{-1} increases. However, during irradiation several new bands occur. The bands at 2092 and 1940 cm^{-1} seem to behave in concert. Both form almost immediately upon irradiation, increase somewhat upon further irradiation, and disappear upon warmup. These bands are provisionally assigned to compound E.

After 25 minutes of irradiation, a new band appears at 2081 cm^{-1} . It does not appear to be associated with compound E, since this band remains upon warming.

Upon warming, new bands appear at 2035, 1985, 1743, and 1737 cm^{-1} . It is not known whether all these bands are associated with the same compound, but they will be referred to as F in further discussion.

Hübel's scheme and its relationship to the results of the experiments described above is of considerable interest. Again, any discussion is hindered by the lack of Hübel's experimental details. Referring again to page 8, two monoacetylene intermediates are invoked. Since neither has any bridging or organic CO groups, they are difficult to detect in a complex reaction mixture. However, the 1885 cm^{-1} band may be due to one of these compounds, more probably $(\text{PhC}_2\text{PhFe}_2(\text{CO})_7)$ since it is the more stable of the two and has been isolated (58). The formation of 2a or 6a has not been observed. The 1677 cm^{-1} band is close to the 1667 cm^{-1} band of 2a, but unlike 2a, is quite stable to photolysis decreasing but slightly during the course of reaction.

When Schrauzer (36) had irradiated diphenylacetylene and iron pentacarbonyl, he used boiling benzene as the solvent. Perhaps the reaction involves an intermediate which only forms at higher temperature, or an activation energy for an excited intermediate to form a new product. At any rate, the expected products have not been found and an explanation will have to await further experiments.

Diphenylacetylene

A sample of diphenylacetylene dissolved in anhydrous ether was placed between two salt plates and cooled to 77°K. The results are summarized in Table 8.

Table 8. Results of irradiation of diphenylacetylene

Conditions	Observations
77°K, before irradiation	Bands observed at 1695 (vw, sh), 1686 (vw), 1675 (vw), 1668 (vw, sh) and 1604 (w) cm^{-1}
77°K, 235 min. irradiation	Intensity increased at 1695 (vw, sh, br), 1686 (vw), and 1675 (vw) cm^{-1}
77°K, 312 min. irradiation	Intensity increased at 1675 (w, sh) cm^{-1}
77°K, after warmup	Intensity decreased at 1695 (vw) and 1675 (vw) cm^{-1}

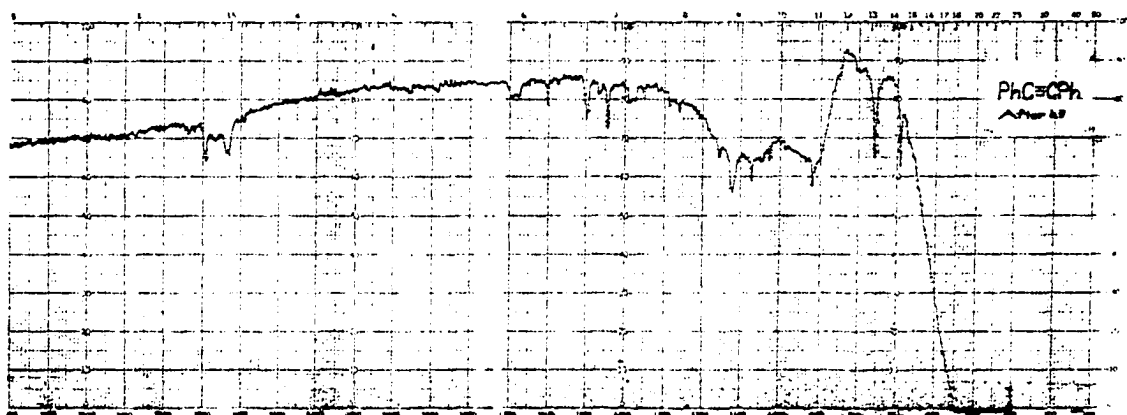
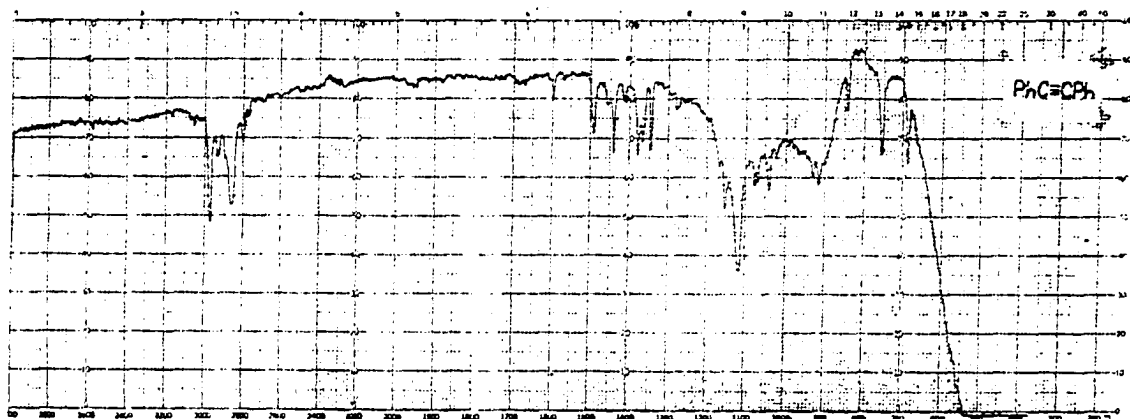
Figures 33-35 show the ir spectra before irradiation, after irradiation, and following warmup, respectively.

This experiment's function was to act as an aid in understanding the results of the runs of diphenylacetylene and $\text{Fe}(\text{CO})_5$. Also, it was hoped that perhaps free cyclobutadiene could be observed. The bands at 1695 and 1675 cm^{-1} did increase somewhat upon irradiation and are consistent with a strained cis double bond found in cyclobutadiene or its dimer. However, the weakness in intensity prohibits a definitive

assignment. The decrease in the 1695 and 1675 cm^{-1} bands on warmup would be consistent with decreased C=C stretching intensity due to dimerization of the cyclobutadiene. One must conclude that little change occurred in the spectra during the course of this experiment.

Figure 33. Diphenylacetylene at 77°K before irradiation

Figure 34. Diphenylacetylene at 77°K after irradiation



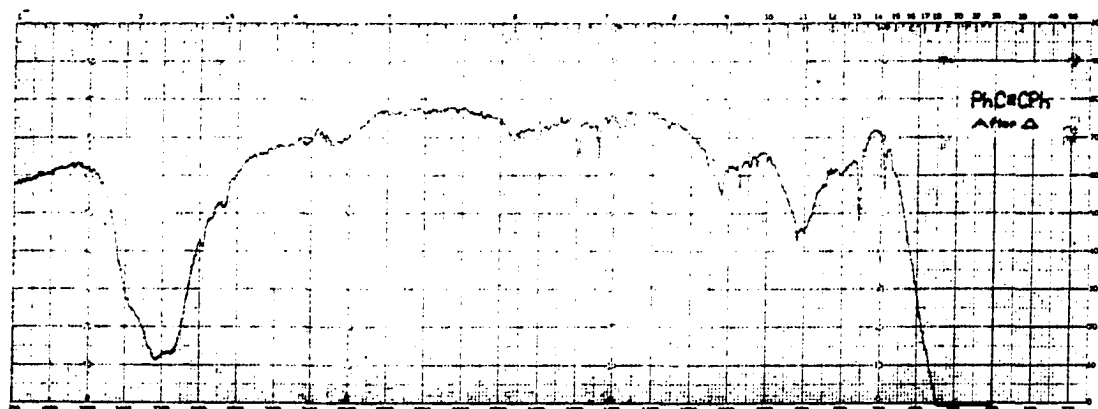


Figure 35. Diphenylacetylene at 77°K following warmup

EXPERIMENTAL

General

Infrared spectra were recorded on a Beckman IR-9, Beckman IR-12, or a Perkin-Elmer Model 21 spectrometer. Nmr spectra were run in carbon tetrachloride or chloroform on a Varian A-60 or Varian HA-100 spectrometer. Melting points are uncorrected and were measured on a Thomas-Hoover capillary melting point apparatus. Mass spectra were obtained on an Atlas CH4 mass spectrometer.

Low Temperature Experiments

The infrared spectra were recorded on either a Beckman IR-9 or IR-12 spectrometer. The light source was an 800 Watt Westinghouse mercury arc lamp focused through one or two quartz focusing lens and then filtered through a Pyrex glass filter if desired.

Two different sets of apparatus were employed. In both cases, a copper constantine thermocouple connected to the cell holder was used. The infrared spectra were analyzed using "IRDATA", a Fortran IV computer program written by the author. (See appendix).

$\text{Fe}(\text{CO})_5$ or solutions containing $\text{Fe}(\text{CO})_5$ were handled and stored in the dark, capped with rubber septa when not in screw top bottles, and transferred by means of syringes.

Method A

The apparatus was based on an earlier design (59) and consisted of an infrared cell, model WXA, obtained from Air Products and Chemicals, Allentown, Pennsylvania. The cell consisted of a vacuum shroud, a cooling unit and a sample holder.

The vacuum shroud was fitted with two sodium chloride windows (0.25 min. by 1.75 in. diameter) and two, septum sealed, gas inlet ports. The sodium chloride windows were sealed to the metal shroud with lubricated Neoprene "o" rings. The vacuum within the shroud securely held the windows in place during operation.

The sample holder consisted of two metal plates, designed to hold the sodium chloride plates, held together by five small screws. The sample holder screwed directly into the base of the cooling vessel parallel to the windows of the vacuum shroud.

The unit was warmed by removing the coolant and then passing a stream of compressed air through the cooling vessel. The sample was placed between two polished sodium chloride plates having an appropriate aluminum spacer and gradually cooled and evacuated until the appropriate temperature and vacuum were reached.

Method B

The apparatus consisted of a Research and Industrial Instruments (RIIC) Model VLT-2 Variable Low Temperature Unit obtained from Beckman Instruments, Fullerton, California. It consisted of a heated cell holder, refrigerant vessel, thermocouple, and sodium chloride windows on an outer vacuum shroud. A Beckman FHOIN sealed, heated infrared cell with sodium chloride windows separated by an appropriate spacer was used. The unit was warmed by removing the coolant and then heating the cell using a RIIC PS-1 Power Supply also obtained from Beckman Instruments.

A sample was placed in the sample cell and sealed with two self-tapping screws. The apparatus was slowly cooled and evacuated until the appropriate temperature was reached.

Iron pentacarbonyl

Method A was employed. A 0.007 mm. spacer, a Pyrex filter, and 2 focusing lenses were used. The $\text{Fe}(\text{CO})_5$ was obtained from Alfa Inorganic and used without further purification.

Table 9. Conditions under which infrared spectra were recorded for $\text{Fe}(\text{CO})_5$

Min.	$^{\circ}\text{K}$	Comment
0	77	
146	77	
146	77	Redone to be on same scale with the rest of the warmup spectra
146	100	
146	110	
146	120	
146	130	
146	140	
146	150	
146	163	
146	181	
146	189	
146	196	
146	202	
146	209	
146	216	
146	224	
146	230	
146	236	
146	242	
146	77	Cooled following warmup

Iron pentacarbonyl and 3-hexyne

In the first of three runs method A was employed using a yellow-orange 2:1 molar mixture of 3-hexyne:iron pentacarbonyl, an 0.025 mm. spacer, a Pyrex filter, and a single focusing lens. After 320 min., the sample warmed while the irradiation continued for 76 min.

Table 10. Conditions when infrared spectra were recorded for first run of 3-hexyne and $\text{Fe}(\text{CO})_5$

Min.	Temp. °K	Comments
0	77	White solid
5	77	
15	77	
45	77	
105	77	Green with black around edges
320	77	A second focusing lens added
396	298	Irradiated while warming

In the second run a 5:1 3-hexyne: $\text{Fe}(\text{CO})_5$ molar mixture was used and method B was followed. A 0.025 mm. spacer, a Pyrex filter, and one focusing lens were employed. A liquid nitrogen-methylene chloride bath was used to maintain a constant temperature.

In the third run a 5:1 molar mixture of 3-hexyne:iron pentacarbonyl was prepared in the dark in a 10 ml. centrifuge tube. The tube was then centrifuged, and the centrifugate was quickly transferred to the apparatus by means of a 50 ul. syringe. Method A was used with 0.025 mm. spacer, a Pyrex filter, and two focusing lenses.

Table 11. Conditions when infrared spectra were recorded for second run of 3-hexyne and $\text{Fe}(\text{CO})_5$

Min.	$^{\circ}\text{K}$	Comments
0	171	
7	171	
12	171	
20	171	
30	171	
39	171	
51	171	
51	171	To get on warmup scale
51	187	
51	195	
51	204	
51	232	
51	243	
51	252	
51	260	
51	269	
51	277	
51	284	
51	296	

Table 12. Conditions when infrared spectra were recorded for third run of 3-hexyne and $\text{Fe}(\text{CO})_5$

Min.	$^{\circ}\text{K}$	Comments
0	77	
5	77	
20	77	
252	77	
629	77	
629	160	Warmup initiated
629	204	
629	224	
629	229	
629	231	
629	237	
629	240	
629	246	
629	248	
629	77	Cooled with Liq. N_2 following warmup

Iron pentacarbonyl and diphenylacetylene

In the first of three runs, a 5:1 molar ratio was prepared by dissolving 0.178 g (0.001 moles) diphenylacetylene (Aldrich Chemical Co.) in 0.5 ml. diethyl ether and adding 0.027 ml. (0.0002 moles) iron pentacarbonyl to form a yellow solution. Method A was employed using a 0.050 mm. aluminum spacer, two quartz lenses, and a Pyrex filter.

Table 13. Conditions when infrared spectra were recorded for the first run of diphenylacetylene and $\text{Fe}(\text{CO})_5$

Min.	$^{\circ}\text{K}$	Comments
0	77	White solid
490	77	Gray-green solid
490	163	
490	169	
490	178	
490	201	
490	214	
490	77	Cooled after warmup

In the second run 0.178 g (0.001 moles) diphenylacetylene were dissolved in 1.00 ml. anhydrous diethyl ether (Malinkrodt) and 0.392 g (0.002 moles) $\text{Fe}(\text{CO})_5$ were added. Method B was used with an 0.1 min. spacer, a Pyrex filter and one or two quartz focusing lens. The temperature was maintained at 173°K by use of a methylene chloride-liquid nitrogen slurry, and at 190°K by means of Dry Ice-acetone bath.

Diphenylacetylene

0.178 g (0.001 moles) diphenylacetylene was dissolved in 0.5 ml anhydrous ether. Method A was employed using a 0.007 mm. spacer, a Pyrex filter and two focusing lenses.

Table 14. Conditions under which the infrared spectra were recorded in the second run of diphenylacetylene and $\text{Fe}(\text{CO})_5$

Min.	$^{\circ}\text{K}$	Comments
0	173	White solid
5	173	One focusing lens employed
10	173	Irradiation started on other face
25	190	Green-white solid
35	190	Green solid
45	190	
60	190	
75	190	Two lenses employed
105	190	
105	209	Warmup begins
105	226	
105	238	
105	249	
105	258	
105	226	
105	289	Light brown solution

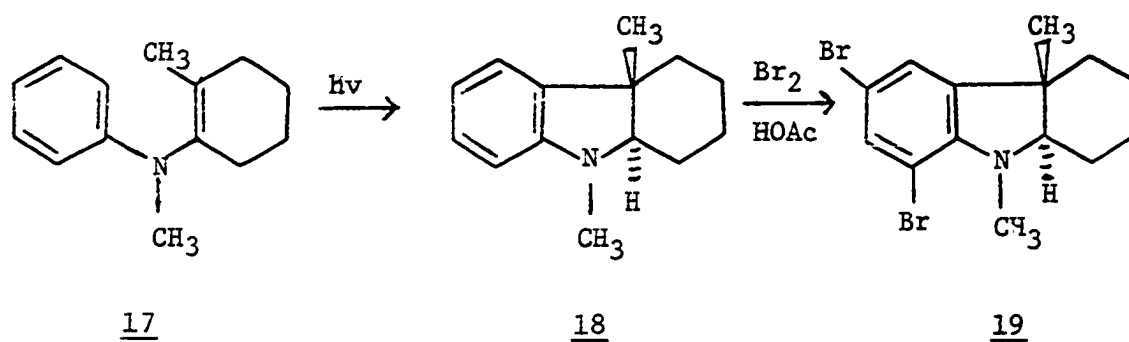
Table 15. Conditions under which infrared spectra were recorded for diphenylacetylene

Min.	$^{\circ}\text{K}$	Comments
0	77	
235	77	
312	77	Remove liq. N_2 , allow to warmup with air stream
312	173	
312	174	
312	182	
312	186	
312	77	Cooled with liq. N_2 following warmup

PART II. THE X-RAY STRUCTURE DETERMINATION OF
TRANS-6,8-DIBROMO-1,2,3,4,4a,9a-HEXAHYDRO-
4a,9-DIMETHYLCARBAZOLE

INTRODUCTION

Chapman and Eian (60) studied the non-oxidative photocyclization of N-aryl enamines and found them to form 2,3-dihydroindoles in high yield in a stereoselective manner. Dr. G. L. Eian kindly supplied a sample of trans-6,8-dibromo-1,2,3,4,4a,9a-hexahydrocarbazole (19) which had been obtained by the series of reactions shown below.



The x-ray structure determination was undertaken in order to confirm the trans- stereochemistry of 19 and to show that the C-methyl group had not migrated. 18 was brominated in order to facilitate the solution of the problem by heavy atom techniques. The presence of the dialkyl amine group led to the increased activation of the benzene ring and the incorporation of 2 Br atoms.

EXPERIMENTAL

A clear, hygroscopic, plate-like crystal of 19 was sealed in a thin-walled Lindemann glass capillary. Preliminary Weissenberg and precession photographs showed the presence of the following systematic absences: $h00$ ($h = 2n + 1$), $0k0$ ($k = 2n + 1$), 00ℓ ($\ell = 2n + 1$), $h0l$ ($h + l = 2n + 1$). The photographs exhibited $2/m$ Laue symmetry indicating a monoclinic space group. The absences are consistent with the space group $P2_1/n$ (C_{2h}^5 ; alternate setting). The unit cell parameters at room temperature are $a = 12.53 \pm 0.02 \text{ \AA}$, $b = 15.88 \pm 0.02 \text{ \AA}$, $c = 7.22 \pm 0.02 \text{ \AA}$ and $95.60 \pm 0.10^\circ$. A calculated density of 1.67 g/cc indicated 4 molecules per unit cell or one molecule per asymmetric unit. An accurate observed density was not obtained because of solubility and decomposition difficulties. For data collection, a crystal having approximate dimensions $0.23 \text{ mm.} \times 0.20 \text{ mm.} \times 0.04 \text{ mm.}$ was selected.

Data were collected at room temperature utilizing an automated Hilger-Watts four circle diffractometer equipped with scintillation counter and using Ni-filtered $\text{CuK}\alpha$ radiation (1.5418 \AA). Within a two-theta sphere of 110° , all data in the hkl and $\bar{h}kl$ octants were recorded using the θ - 2θ scan technique with a take off angle of 8° .

As a general check on electronic and crystal stability, the intensities of three standard reflections were measured periodically during the data collection. No significant change in intensity was observed. The absorption coefficient for Cu radiation is 48 cm^{-1} , and an absorption correction was judged to be necessary. The standard deviations of the intensity, $\sigma[I]$, were estimated by use of $\sigma[I] =$

$$\sqrt{[\text{total count}] + [\text{background}] + \left[\frac{5^\circ}{100} \text{ total count} \right]^2 + \left[\frac{5^\circ}{100} \text{ background} \right]^2}.$$

Of the 1806 reflections measured, 1444 had $I > 3\sigma[I]$ and these were considered observed and were used in the refinement. The intensities were corrected for Lorentz and polarization factors to give F_o^2 .

A three-dimensional Patterson synthesis was computed from the observed data (61). The positions of the two independent bromine atoms were obtained from this synthesis. The remaining non-hydrogen atoms were found by successive structure factor calculations and electron density syntheses. The positions were refined by full matrix least-squares techniques with anisotropic thermal parameters for all atoms to a conventional discrepancy index $[R = \sum |F_o| - |F_c|] / \sum F_o]$ of 0.089 and a weighted R-factor $[wR = [\sum w [|F_o| - |F_c|]^2 / \sum w |F_o|^2]^{1/2}]$ of the 0.119 (62). The w's were calculated from σ_{F_o} 's for each reflection (63) by means of $\sigma_{F_o} = \sqrt{F_o^2 + \sigma[I]^2} / LP - F_o$. The scattering factors were those of Hanson, et al. (64).

A final electron density difference map showed no peaks greater than $0.4 e/\text{\AA}^3$. No unusual trends in F_o and F_c values were found and the weighting scheme was judged to be a reasonable one.

A series of tables and figures follow. In Tables 16 and 17, the final values of the positional parameters and anisotropic thermal parameters are listed. Final intramolecular bond distances and angles along with their standard deviations as derived from the inverse matrix (65) are presented in Tables 18 and 19. Table 20 gives the values of $10F_o$ and $10F_c$ while Tables 21 and 22 show the results of mean plane calculations. A drawing of the molecule including anisotropic thermal motion (66) is presented in Figure 35.

Table 16. Final fractional coordinates

Atom	<u>x</u>	<u>y</u>	<u>z</u>
C(1)	0.2361(4) ^a	-0.2104(6)	0.8538(6)
C(2)	0.1735(6)	-0.1629(6)	0.0063(4)
C(3)	0.0845(5)	-0.1005(2)	0.9328(8)
C(4)	0.1269(4)	-0.0364(2)	0.7874(2)
C(4a)	0.1797(7)	-0.0875(7)	0.6379(9)
C(5)	0.2126(1)	0.0355(0)	0.4033(7)
C(5a)	0.2418(7)	-0.0373(0)	0.5004(4)
C(6)	0.2765(5)	0.0591(1)	0.2687(8)
C(7)	0.3673(2)	0.0153(8)	0.2222(3)
C(8)	0.3966(6)	-0.0587(5)	0.3266(2)
C(8a)	0.3359(8)	-0.0871(8)	0.4690(0)
N(9)	0.3401(7)	-0.1587(6)	0.5834(1)
C(9a)	0.2765(9)	-0.1372(8)	0.7358(2)
C(10)	0.4463(9)	-0.1993(7)	0.6391(5)
C(11)	0.0989(0)	-0.1462(3)	0.5237(8)
Br(12)	0.5123(4)	-0.1200(1)	0.2448(5)
Br(13)	0.2418(3)	0.1601(1)	0.1293(1)

^aEstimated standard deviations for coordinates given in parentheses .

Table 17. Final thermal parameters^a

Atom	β_{11}	β_{22}	β_{33}	β_{12}	β_{13}	β_{23}
C(1)	0.0132(2) ^b	0.0067(5)	0.0399(2)	-0.0007(6)	0.0041(0)	0.0059(9)
C(2)	0.0136(9)	0.0095(6)	0.0289(2)	-0.0021(4)	0.0048(8)	-0.0003(3)
C(3)	0.0128(2)	0.0085(7)	0.0318(6)	0.0016(2)	0.0044(7)	0.0032(5)
C(4)	0.0128(9)	0.0079(4)	0.0288(2)	0.0010(0)	0.0041(4)	-0.0004(8)
C(4a)	0.0092(9)	0.0056(6)	0.0251(1)	0.0005(8)	0.0037(3)	0.0007(3)
C(5)	0.0109(3)	0.0045(5)	0.0315(9)	-0.0011(2)	0.0037(4)	0.0005(0)
C(5a)	0.0103(9)	0.0047(8)	0.0276(3)	-0.0000(8)	0.0025(2)	-0.0010(0)
C(6)	0.0112(7)	0.0044(5)	0.0403(5)	-0.0011(3)	-0.0007(8)	0.0005(2)
C(7)	0.0113(8)	0.0048(4)	0.0370(5)	-0.0018(3)	0.0025(1)	-0.0016(5)
C(8)	0.0088(7)	0.0068(8)	0.0349(9)	-0.0012(3)	0.0072(2)	-0.0036(9)
C(8a)	0.0091(8)	0.0049(4)	0.0341(9)	-0.0003(0)	0.0007(1)	-0.0015(6)
N(9)	0.0107(4)	0.0051(3)	0.0321(4)	0.0005(6)	0.0022(3)	0.0008(2)
C(10)	0.0099(5)	0.0079(5)	0.0467(3)	0.0012(1)	-0.0009(6)	0.0021(8)
C(11)	0.0094(8)	0.0060(3)	0.0336(8)	-0.0004(8)	-0.0003(4)	-0.0005(5)
Br(12)	0.0132(4)	0.0106(7)	0.0531(9)	0.0023(9)	0.0102(6)	0.0003(4)
Br(13)	0.0154(0)	0.0059(9)	0.0430(4)	-0.0011(6)	0.0020(2)	0.0033(3)

^aThe form of the anisotropic temperature factor is $\exp(-[\beta_{11}h^2 + \beta_{22}k^2 + \beta_{33}l^2 + 2\beta_{12}hk + 2\beta_{13}hl + 2\beta_{23}kl])$.

^bEstimated standard deviations for coordinates given in parentheses.

Table 18. Selected bond distances

Atom	Atom	Distance (Å)
C(1)	C(2)	1.600 (0.021) ^a
C(1)	C(9a)	1.554 (0.017)
C(2)	C(3)	1.547 (0.021)
C(3)	C(4)	1.590 (0.018)
C(4)	C(4a)	1.549 (0.016)
C(4a)	C(5a)	1.542 (0.015)
C(4a)	C(9a)	1.557 (0.016)
C(4a)	C(11)	1.552 (0.016)
C(5)	C(5a)	1.382 (0.015)
C(5)	C(6)	1.370 (0.017)
C(5a)	C(8a)	1.456 (0.016)
C(6)	C(7)	1.402 (0.017)
C(6)	Br(13)	1.920 (0.013)
C(7)	C(8)	1.425 (0.017)
C(8)	C(8a)	1.410 (0.017)
C(8)	Br(12)	1.887 (0.012)
C(8a)	N(9)	1.403 (0.015)
N(9)	C(9a)	1.460 (0.016)
N(9)	C(10)	1.498 (0.016)
C(10)	Br(12)	3.289 (0.017)

^aStandard deviations obtained from ORFFE in parentheses.

Table 19. Selected bond angles

Atom	Atom	Atom	Angle (°)
C(1)	C(2)	C(3)	116.8 (1.1) ^a
C(1)	C(9a)	C(4a)	110.2 (1.0)
C(1)	C(9a)	N(9)	117.9 (1.0)
C(2)	C(3)	C(4)	111.1 (1.1)
C(2)	C(1)	C(9a)	103.4 (1.0)
C(3)	C(4)	C(4a)	108.4 (1.0)
C(4)	C(4a)	C(5a)	109.6 (1.0)
C(4)	C(4a)	C(9a)	108.4 (0.9)
C(4)	C(4a)	C(11)	112.5 (1.0)
C(4a)	C(5a)	C(5)	129.2 (1.0)
C(4a)	C(5a)	C(8a)	106.6 (0.9)
C(4a)	C(9a)	N(9)	103.6 (0.8)
C(5)	C(5a)	C(8a)	123.6 (1.0)
C(5)	C(6)	C(7)	125.3 (1.1)
C(5)	C(6)	Br(13)	118.7 (1.0)
C(5a)	C(4a)	C(9a)	97.7 (0.8)
C(5a)	C(4a)	C(11)	108.2 (0.9)
C(5a)	C(5)	C(6)	116.3 (1.1)
C(5a)	C(8a)	C(8)	116.2 (1.0)
C(5a)	C(8a)	N(9)	112.2 (1.1)
C(6)	C(7)	C(8)	117.1 (1.1)
C(7)	C(6)	Br(13)	115.8 (1.0)
C(7)	C(8)	C(8a)	121.2 (1.1)
C(7)	C(8)	Br(12)	115.2 (0.8)
C(8)	C(8a)	N(9)	134.1 (1.1)
C(8a)	C(8)	Br(12)	123.2 (1.0)
C(8a)	N(9)	C(9a)	105.1 (0.9)
C(8a)	N(9)	C(10)	119.2 (1.0)
C(9a)	N(9)	C(10)	115.7 (1.0)

^aStandard deviations obtained from ORFFE in parentheses.

Table 21. Deviations from mean plane of benzene ring

Atom	Perpendicular distance to plane (Å)
C5a	-0.01
C5	0.00
C6	0.01
C7	-0.01
C8	0.00
C8a	0.01
C4a	-0.22
N9	-0.07
C9a	0.39
C10	0.49
Br12	0.17
Br13	0.04

Table 22. Deviations from mean plane of C4a-C5a-C8a-N9

Atom	Perpendicular distance to plane (Å)
C4a	-0.01
C5a	0.02
C8a	-0.02
N9	0.01
C9a	0.62
C10	0.55
C5	-0.05
C6	-0.21
C7	-0.30
C8	-0.19

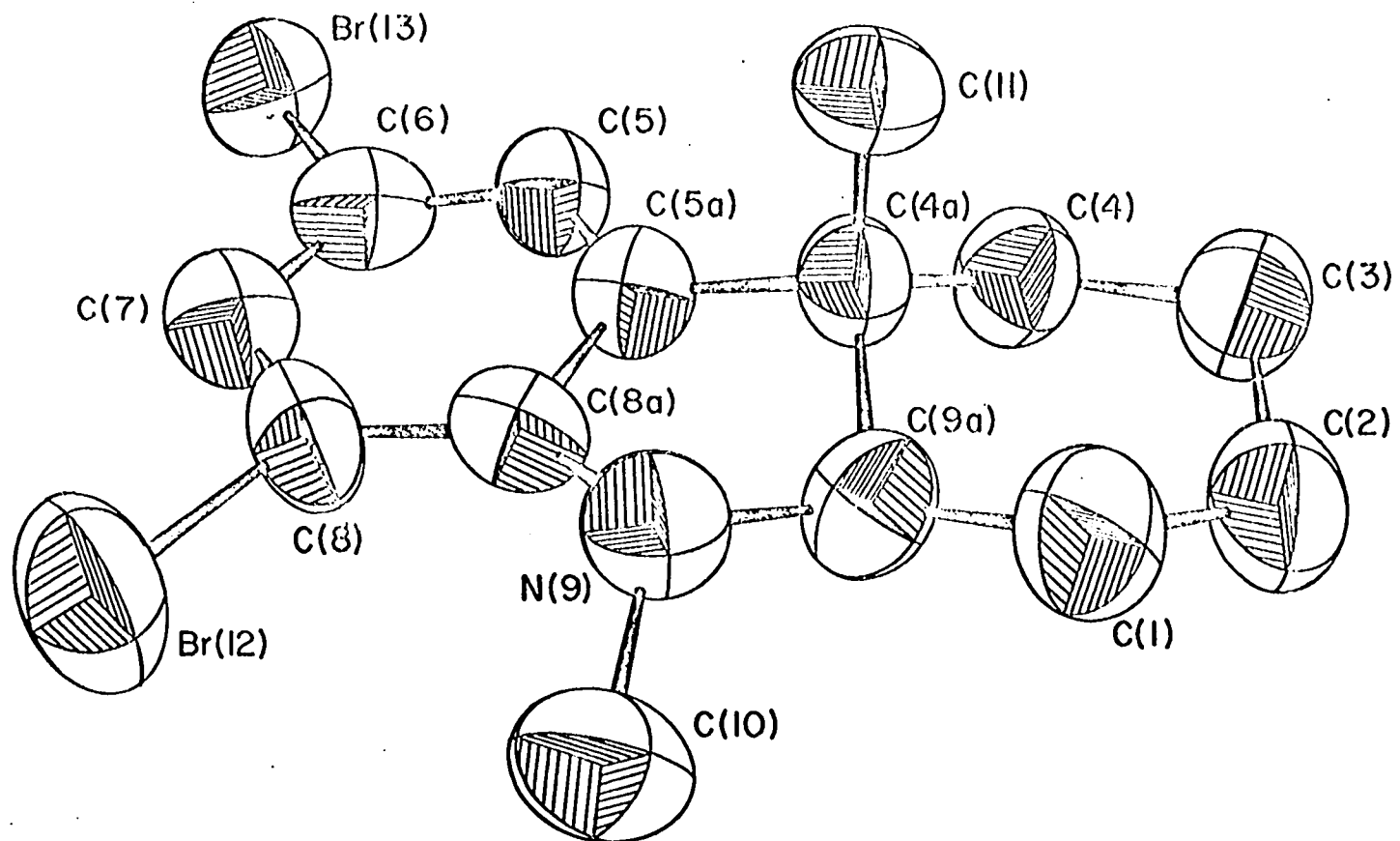


Figure 36. Computer drawing of *trans*-6,8-bromo-4a,9-dimethyl-1,2,3,4,4a,9a-hexahydrocarbazole including 50% anisotropic thermal motion

DISCUSSION

The trans stereochemistry at the 6-5 ring fusion is confirmed by the structure determination. The heterocyclic ring is diequatorial to the cyclohexane with the observation that the N9-C9a-C4a-C5a torsional angle of $71.42 \pm 1.27^\circ$ is somewhat more open than the ideal angle of 60° . The C1-C2 and C3-C4 bond distances are somewhat longer than expected. However, the deviation from the expected distance (67) of 1.53 \AA could be caused by the skewing of the anisotropic thermal parameters to account for the C-H bond electron densities and perhaps by some motion of the carbon skeleton. Some variation in the cyclohexane C-C-C bond angles occur from the accepted value (67) of 111.6° . However, calculations (68) have shown that small variations in bond angles to overcome torsional strain are low energy processes.

Serious steric interaction occurs between Br12 and C10. The intermolecular distance of 3.46 \AA is considerably shorter than the van der Waals distance of 3.95 \AA (69). The response to this interaction is a displacement of C10 out of the plane of the benzene ring. The dihedral angle between C10-N9-C9a and C8-C8a-C5a is $139.89 \pm 1.44^\circ$. Evidently the nitrogen atom is tetrahedrally hybridized.

The electronic and steric requirements have destroyed the equivalent 1.392 \AA C-C distances (70) found in benzene. The C7-C8 and C5a-C8a distances are somewhat elongated and the ring angles about C5a, C6 and C8 have opened up from the idealized 120° while the other three benzene ring bond angles have contracted. However, the average bond length of 1.408 \AA and the average bond angle is 119.33° , both are quite reasonable and well within experimental uncertainty. The benzene ring remains planar,

but Br12, and C4a are clearly somewhat out of this plane. Generally small deviations from planarity require little energy. Although N9 is only 0.07 Å out of the plane of the benzene ring, both C10 and C9a are further removed from the plane and N9 is not sp^2 hybridized.

The heterocyclic ring is in an envelope conformation C_s symmetry, with the C4a-C5a-C8a-N9 fragment planar. The C9a atom forms the "flap" of the envelope and is bent away from C11. The requirements of the trans 6-5 ring fusion, the two sp^2 carbons and the van der Waals interaction of C10 and Br12 contribute to considerable distortion of the central ring bond angles. C10 is in an equatorial position trans to C1 and C11 and cis to C4a. Finally, C11 has not migrated during the photochemical reaction.

LITERATURE CITED

1. M. Berthelot, *Compt. Rend.*, 112, 1343 (1891).
2. L. Mond and F. Quincke, *J. Chem. Soc.*, 604 (1891).
3. R. H. Herber, W. K. Kingston and G. K. Wertheim, *Inorg. Chem.*, 2, 153 (1963)
4. H. Stammreich, O. Sala and Y. Tavares, *J. Chem. Phys.*, 30, 856 (1959).
5. G. Bor, *Inorg. Chim. Acta*, 3, 191 (1969).
6. A. Reckziegel and M. Bigorgne, *J. Organometallic Chem.*, 3, 341 (1965).
7. L. H. Jones and R. S. McDowell, *Spectrochim Acta*, 20, 248 (1964).
8. W. F. Edgell, W. E. Wilson and R. Summitt, *Spectrochim Acta*, 19, 863 (1963).
9. R. K. Sheline and K. S. Pitzer, *J. Amer. Chem. Soc.*, 72, 1107 (1950).
10. A. W. Hanson, *Acta Crystallogr.*, 15, 930 (1962).
11. J. Donohue and A. Caron, *Acta Crystallogr.*, 17, 663 (1964).
12. R. V. G. Evans and M. W. Lister, *Trans. Faraday Soc.*, 35, 631 (1939).
13. M. I. Davis and H. P. Hanson, *J. Phys. Chem.*, 69, 3405 (1965).
14. J. Donohue and A. Caron, *J. Phys. Chem.*, 70, 603 (1966).
15. M. I. Davis and H. P. Hanson, *J. Phys. Chem.*, 71, 775 (1967).
16. J. Donohue and A. Caron, *J. Phys. Chem.*, 71, 777 (1967).
17. B. Beagley, D. W. J. Cruickshank, P. M. Pindar, A. G. Robiette and G. M. Sheldrick, *Acta Crystallogr.*, B, 25, 737 (1969).
18. A. Almeningen, A. Hoaland and K. Wahl, *Acta Chem. Scand.*, 23, 2245 (1969).
19. A. F. Schreiner and T. L. Brown, *J. Amer. Chem. Soc.*, 90, 3366 (1968).
20. F. A. Cotton, A. Danti, J. S. Waugh and R. W. Fessenden, *J. Chem. Phys.*, 29, 1427 (1958).

21. R. Bramley, B. N. Figgis and R. S. Nyholm, *Trans. Faraday Soc.*, 58, 1893 (1962).
22. R. S. Berry, *J. Chem. Phys.*, 32, 933 (1960).
23. L. R. Kangas, R. F. Heek, P. M. Henry, S. Breitschaft, E. M. Thorsteinson and F. Basolo, *J. Amer. Chem. Soc.*, 88, 2334 (1966).
24. D. F. Keeley and R. E. Johnson, *J. Inorg. Nucl. Chem.*, 11, 33 (1959).
25. K. Noack and M. Ruch, *J. Organometallic Chem.*, 17, 309 (1969).
26. C. A. Udovich, R. J. Clark and H. Haas, *Inorg. Chem.*, 8, 1066 (1969).
27. J. Dewar and H. O. Jones, *Proc. Royal Soc. London, A*, 79, 66 (1906).
28. G. Eyber, *Z. Physik. Chem., A*, 144, 1 (1929).
29. I. W. Stolz, G. R. Dobson and R. K. Sheline, *J. Amer. Chem. Soc.*, 84, 3589 (1962).
30. I. W. Stolz, G. R. Dobson and R. K. Sheline, *J. Amer. Chem. Soc.*, 85, 1013 (1963).
31. F. C. Bowden and A. B. P. Lever, *Organometallic Chem. Rev., A*, 3, 1 (1968).
32. W. Hübel, "Organometallic Derivatives from Metal Carbonyls and Acetylene Compounds", in I. Wender and P. Pino, eds., "Organic Syntheses via Metal Carbonyls", Vol. 1, Interscience Publishers, New York, N.Y., 1968, pp. 273-342.
33. W. Reppe and H. Vetter, *Ann.*, 582, 133 (1953).
34. J. R. Case and M. C. Whiting, *J. Chem. Soc.*, 4632 (1962).
35. E. Weiss, R. Merenyi and W. Hübel, *Chem. Ind.*, 407 (1960).
36. G. N. Schrauzer, *J. Amer. Chem. Soc.*, 81, 5307 (1959).
37. E. H. Braye, C. Hoogzand, W. Hübel, U. Krüerke, R. Merenyi and E. Weiss, in S. Kirschner, ed., "Advances in the Chemistry of the Coordination Compounds", p. 190, Macmillan, New York, N.Y., 1961.
38. H. W. Sternberg, R. A. Friedel, R. Markby and I. Wender, *J. Amer. Chem. Soc.*, 80, 1009 (1958).
39. J. F. Blount, L. F. Dahl, C. Hoogzand and W. Hübel, *J. Amer. Chem. Soc.*, 88, 292 (1966).

40. W. Hübel and E. H. Braye, *J. Inorg. Nucl. Chem.*, 10, 250 (1959).
41. E. H. Braye and W. Hübel, *J. Organometallic Chem.*, 3, 38 (1965).
42. R. S. Dickson and D. B. W. Young, *Aust. J. Chem.*, 21, 97 (1968).
43. R. S. Dickson and D. B. W. Young, *Aust. J. Chem.*, 21, 97 (1968).
44. G. Wilkinson, *J. Chem. Soc.*, 3488 (1962).
45. E. Weiss, W. Hübel and R. Merenyi, *Chem. Ber.*, 95, 1155 (1962).
46. M. Rosenblum, N. Brown and B. King, *Tetrahedron Lett.*, 4421 (1967).
47. E. H. Braye, L. F. Dahl, W. Hübel, and D. L. Wampfler, *J. Amer. Chem. Soc.*, 84, 4633 (1962).
48. E. H. Braye and W. Hübel, *J. Organometallic Chem.*, 3, 25 (1965).
49. L. F. Dahl, R. J. Doedens, W. Hübel, and J. Nielson, *J. Amer. Chem. Soc.*, 88, 446 (1966).
50. C. Hoogzand and W. Hübel, *Proc. Eighth Intern. Conf. Coordination Chem.*, Vienna, 1964, p. 258.
51. W. Hübel, *op. cit.*, p. 287.
52. C. W. Bird, E. M. Briggs, and J. Hudec, *J. Chem. Soc.*, C, 1862 (1967).
53. L. E. Orgel, "Special Publication 13", The Chemical Society, London, 1959, p. 93.
54. W. Strohmeier, *Angew. Chem. Int. Ed. Engl.*, 3, 730 (1964).
55. E. H. Schubert and R. K. Sheline, *Inorg. Chem.*, 5, 1071 (1966).
56. J. Lassila and J. Buss, personal communication, 1969.
57. S. McVey and P. M. Maitlis, *Can. J. Chem.*, 44, 2429 (1966).
58. W. Hübel, *op. cit.*, p. 277.
59. E. L. Wagner and D. F. Hornig, *J. Chem. Phys.*, 18, 296 (1950).
60. O. L. Chapman and G. L. Eian, *J. Amer. Chem. Soc.*, 90, 5329 (1968).
61. J. Rodgers and R. A. Jacobson, "ALF, A General Fourier Program in PLI for Triclinic, Monoclinic, and Orthorhombic Space Groups", U. S. Atomic Energy Commission Report IS-2155 (Iowa State University, Ames, Iowa, 50010), 1969.

62. W. R. Busing, K. O. Martin, and H. A. Levy, "ORFLS, A Fortran Crystallographic Least-Squares Program", ORNL-TM-305 (The Oak Ridge National Laboratory, Oak Ridge, Tennessee), 1962.
63. D. E. Williams and R. E. Rundle, J. Amer. Chem. Soc., 86, 1660 (1964).
64. H. P. Hanson, F. Mermon, J. D. Lee, and S. Skillman, Acta Crystallogr., 17, 1040 (1964).
65. W. R. Busing, K. O. Martin, and H. A. Levy, "ORFFE, A Fortran Function and Error Program", ORNL-TM-306 (The Oak Ridge National Laboratory, Oak Ridge, Tennessee), 1962.
66. C. K. Johnson, "ORTEP, A Fortran Thermal-Ellipsoid Plot Program for Crystal Structure Illustrations", ORNL-3794 (The Oak Ridge National Laboratory, Oak Ridge, Tennessee), 1965.
67. E. L. Eliel, N. L. Allinger, S. J. Angyal, and G. A. Morrison, "Conformational Analysis", Interscience Publishers, New York, N.Y., 1965, p. 455.
68. E. L. Eliel, N. L. Allinger, S. J. Angyal, and G. A. Morrison, "Conformational Analysis", Interscience Publishers, New York, N.Y., 1965, p. 456.
69. L. Pauling, "The Nature of the Chemical Bond", 3rd Ed., Cornell University Press, Ithaca, N.Y., 1960, p. 260.
70. A. F. Wells, "Structural Inorganic Chemistry", 3rd Ed., Oxford University Press, London, 1962, p. 711.

ACKNOWLEDGMENTS

The author wishes to acknowledge the patience, understanding and guidance of Professor O. L. Chapman whose encouragement enabled the author to develop his interest in crystallography and whose suggestions led to the research in this thesis.

The author's introduction to crystallography was made possible by Professor Robert Jacobson's aid and encouragement. Professor Jon Clardy was instrumental in the solution of the crystal structure included in this dissertation. Much of the author's practical knowledge of crystallography was gained through the help of Mr. Fred Hollenbeck, Mr. Les Martin, Dr. James Rodgers and Mr. Marv Hackert.

The author also wishes to acknowledge the helpful discussions with Professor R. J. Angelici.

Much of the author's early enthusiasm for chemistry was sparked by Professor Paul Haberfield of Brooklyn College.

The drafts of this thesis were executed by the author's wife, Jackie, and the final copy was typed by Mrs. Louise Dayton. Dr. C. L. McIntosh was very helpful in getting the figures reproduced.

Finally, the author faces the impossible task of thanking his parents for their love and support and his wife for responding to the many frustrations and hardships with constant love and encouragement.

APPENDIX

In order to organize the data obtained from the many infrared spectra a Fortran IV program, "IRDATA", was written by the author. Dr. C. L. McIntosh assisted in putting the program in its final form. The program takes the band, base line intensity, transmitted intensity, and standard band(s), as well as the time and temperature at which each spectrum was recorded, and computes the absorbancy, corrected with each standard band's absorbancy and averaged for all the standard bands in the run. If no standard bands are included, the absorbancy of each band is still calculated, but no correction is made. Also printed out is a sorted list of all the bands observed in a particular run as well as a table of the band and its absorbancy in each spectrum of the run. A listing of the program follows.

```

//C418BCLM JOB 'A0332,REGION=128K,TIME=2', C MCINTOSH
//S1 EXEC FORTGCG,REGION=128K
//FORT.SYSIN DD *
C THIS PROGRAM HANDLES IR DATA OBTAINED FROM FOLLOWING A REACTION
C     IF LPNCH=0, NO CARDS WILL BE PUNCHED; IF 1, CARDS PUNCHED FOR TIME& ABS
C     IF=2, CARDS PUNCHED FOR TEMP & ABS; IF =3, BOTH SETS OF CARDS PUNCHED
C     IF MTBL (POSITION 15 ON CARD 2) IS EG THAN 1 A TABLE OF RUN VERSUS
C     BAND WILL BE PRINTED AT TH END
C     THIS PROGRAM WILL HANDLE UP TO 80 BANDS AND 50 RUNS.
      DIMENSION SIO(50),AI(50),FACTOR(50),SI(50),SBAND(50),ACOR(50),AAC(
150),ASTAND(50),TITLE(20),TIME(50),TEMP(50),NBANDS(50),BAND(50,50),
2AFNL(50,80),A(50),BLIST(301),TBAND(50),CLIST(80),LPNCH(50)
      COMMON BLIST,NRUNS,NBANDS,BAND,TIME,TEMP,CLIST,AFNL
901 N=0
      LIST=0
      READ(1,300)TITLE
      WRITE(3,350)TITLE
      READ(1,255)ISENT,NRUNS,MTLB
20 N=N+1
      IF(N.GT.NRUNS)GO TO 15
      READ(1,700)TIME(N),TEMP(N),AIO,NBANDS(N),NSTAND,LPNCH(N)
      LN=NBANDS(N)
      DO 711 I=1,LN
711 AAC(I)=0.
      IF(NSTAND.EQ.0) GO TO 99
      DO 162 J=1,NSTAND
      READ(1,160)SBAND(J),SIO(J),SI(J)
162 ASTAND(J)=ALOG10(SIO(J)/SI(J))
      GO TO 98
99 NSTAND=1
      SBAND(1)=0.
      FACTOR(1)=1.
98 DO 2 I=1,LN
      READ(1,105)BAND(N,I),AI(I)
      A(I)=ALOG10(AIO/(AI(I)))
      DO 81 J=1,NSTAND
      IF(BAND(N,I).EQ.SBAND(J))GO TO 3

```

```
      GO TO 81
      3 FACTOR(J)=ASTAND(J)/A(I)
      81 CONTINUE
      2 CONTINUE
      17 WRITE(3,150)
         WRITE(3,155)TIME(N),TEMP(N),AIO
         DO 8 J=1,NSTAND
            WRITE(3,750)SBAND(J)
            DO 4 I=1,LN
               ACOR(I)=A(I)* FACTOR(J)
               AAC(I)=AAC(I) + ACOR(I)
            4 WRITE(3,200)BAND(N,I),ACOR(I),A(I),FACTOR(J)
            8 CONTINUE
            DO 3001 I=1,LN
               AFNL(N,I)=AAC(I)/NSTAND
               WRITE(3,410)BAND(N,I),AFNL(N,I)
      3001 CONTINUE
         IF(N.EQ.1)GO TO 1004
         K=0
         M=0
         LN=NBANDS(N)
         DO 1002 I=1,LN
            K=0
            DO 1001 J=1,LIST
```



```

        IF(BLIST(J).NE.BAND(N,I))GO TO 1001
        K=K+1
1001 CONTINUE
        IF(K.EQ.1) GO TO 1002
        M=M+1
        TBAND(M)=BAND(N,I)
1002 CONTINUE
        IF(M.EQ.0)GO TO 1005
        KOUNT=M
        DO 1003 M=1,KOUNT
        LIST=LIST + 1
        J=LIST
1003 BLIST(J)=TBAND(M)
1005 GO TO 20
1004 LIST=NBANDS(N)
        LN=NBANDS(N)
        DO 1006 I=1,LN
1006 BLIST(I)=BAND(N,I)
        GO TO 20
15 CONTINUE
        IF(LIST.GT.80)GO TO 87
        CALL DBSRT(LIST,BLIST)
        WRITE(3,3305)
        WRITE(3,3300)(BLIST(J),J=1,LIST)
        DO 4002 J=1,LIST
        DO 4002 N=1,NRUNS
        IPNCH=LPNCH(N)
        IF(LPCH(N).EQ.0)GO TO 4002
        L=0
        LN=NBANDS(N)
        DO 4002 I=1,LN
        IF(BLIST(J).NE.BAND(N,I)) GO TO 4001
        L=L+1

```

```
      GO TO (7001,7002,7003),IPNCH
7001 WRITE(2,7010)TIME(N),AFNL(N,I),BLIST(J),TEMP(N)
      GO TO 4002
7002 WRITE(2,7010)TEMP(N),AFNL(N,I),BLIST(J),TIME(N)
      GO TO 4002
7003 WRITE(2,7010)TEMP(N),AFNL(N,I),BLIST(J),TIME(N)
      WRITE(2,7010)TIME(N),AFNL(N,I),BLIST(J),TEMP(N)
      GO TO 4002
4001 IF(I.NE.LN) GO TO 4002
      IF(L.EQ.1) GO TO 4002
      BFNL=0.0000
      GO TO (7004,7005,7006),IPNCH
7004 WRITE(2,7100)TIME(N),BFNL,BLIST(J),TEMP(N)
      GO TO 4002
7005 WRITE(2,7100)TEMP(N),BFNL,BLIST(J),TIME(N)
      GO TO 4002
7006 WRITE(2,7100)TEMP(N),BFNL,BLIST(J),TIME(N)
      WRITE(2,7100)TIME(N),BFNL,BLIST(J),TEMP(N)
4002 CONTINUE
      401 WRITE(3,2030)TITLE
          WRITE(3,2010)
          DO 2032 N=1,NRUNS
2032 WRITE(3,2031)N,TIME(N),TEMP(N)
          IF(MTLB.EQ.0)GO TO 9999
          IF(LIST.LE.10)GO TO 9998
          K=1
          L=10
          CALL TABLE(K,L)
```

```
IF(LIST.LE.20) GO TO 9997
K=11
L=20
CALL TABLE(K,L)
IF(LIST.LE.30)GO TO 9996
K=21
L=30
CALL TABLE(K,L)
IF(LIST.LE.40)GO TO 9995
K=31
L=40
CALL TABLE(K,L)
IF(LIST.LE.50)GO TO 8995
K=41
L=50
CALL TABLE(K,L)
IF(LIST.LE.60)GO TO 8996
K=51
L=60
CALL TABLE(K,L)
IF(LIST.LE.70)GO TO 8997
K=61
L=70
CALL TABLE(K,L)
K=71
L=LIST
CALL TABLE(K,L)
```

```

      GO TO 9999
8995 K=41
      L=LIST
      CALL TABLE(K,L)
      GO TO 9999
8996 K=51
      L=LIST
      CALL TABLE(K,L)
      GO TO 9999
8997 K=61
      L=LIST
      CALL TABLE(K,L)
      GO TO 9999
      87 WRITE(3,75)LIST
      GO TO 9999
9998 K=1
      L=LIST
      CALL TABLE(K,L)
      GO TO 9999
9997 K=11
      L=LIST
      CALL TABLE(K,L)
      GO TO 9999
9996 K=21
      L=LIST
      CALL TABLE(K,L)
      GO TO 9999
9995 K=31
      L=LIST
      CALL TABLE(K,L)
      GO TO 9999
9999 IF(ISENT.EQ.1)GO TO 901
      105 FORMAT(2F10.3)
      150 FORMAT('    TIME(MIN)          TEMP(K)          ST BAND          BAND

```

```

1 ABSORBANCE          UNCORABSOR          AO          FACTOR          AFNL
2')
75 FORMAT('1 LIST GREATER THAN 80',/,2X,'LIST IS',I5)
155 FORMAT(' ',1X,F10.3,4X,F10.3,63X,F10.3)
160 FORMAT(3F10.3)
200 FORMAT(' ',44X,F10.3,4X,F10.5,4X,F10.5,18X,F10.3)
255 FORMAT(3I5)
300 FORMAT(20A4)
350 FORMAT('1',20A4)
410 FORMAT(' ',44X,F10.3,59X,F10.5)
650 FORMAT(' ',44X,F10.3,17X,F10.5)
700 FORMAT(3F10.3,3I5)
750 FORMAT(' ',29X,F10.3)
2010 FORMAT('0 RUN TIME(MIN) TEMP(K) ')
2030 FORMAT('0',20A4)
2031 FORMAT(' ',I5,2F10.3)
3305 FORMAT('1','COMPILED LIST IS')
3300 FORMAT(' ',10F10.4,/)
7010 FORMAT(4F10.4)
7100 FORMAT(4F10.4)
STOP
END

```

```

SUBROUTINE TABLE(K,L)
DIMENSION SIO(50),AI(50),FACTOR(50),SI(50),SBAND(50),ACOR(50),AAC(
150),ASTAND(50),TITLE(20),TIME(50),TEMP(50),NBANDS(50),BAND(50,50),
2AFNL(50,80),A(50),BLIST(301),TBAND(50),CLIST(80),LPNCH(50)
COMMON BLIST,NRUNS,NBANDS,BAND,TIME,TEMP,CLIST,AFNL
WRITE(3,800) (BLIST(J),J=K,L)
DO 9900 N=1,NRUNS
LN=NBANDS(N)
DO 9800 J=K,L
M=0
DO 9800 I=1,LN
IF(BLIST(J).NE.BAND(N,I))GO TO 9801
M=M+1
CLIST(J)=AFNL(N,I)
GO TO 9800
9801 IF(I.NE.LN)GO TO 9800
IF(M.EQ.1)GO TO 9800
CLIST(J)=0.
9800 CONTINUE
WRITE(3,810)TIME(N),TEMP(N),(CLIST(J),J=K,L)
9900 CONTINUE
800 FORMAT(1H1,/,/, ' TIME TEMP ',10F10.1)
810 FORMAT(' ',12F10.4)
RETURN
END
40
//LKED.SYSLIB DD DSNAME=SYS1.MATHLIB,DISP=SHR
// DD DSNAME=SYS1.FORTLIB,DISP=SHR
//GO.SYSIN DD *

```

VITA

The author, son of Mr. and Mrs. Saul Bloom, was born in New York on September 9, 1943. He was raised in Brooklyn, New York where he attended the public school system, graduating from Brooklyn Technical High School in June, 1961. He entered Brooklyn College the following September with a New York State Regents' College Scholarship, and graduated in June, 1965 with a B.S. in chemistry. The author was a National Science Foundation Undergraduate Research Participant for two years under the supervision of Professor Paul Haberfield.

In September, 1965 the author entered Iowa State University of Science and Technology where he was directed by Professor O. L. Chapman, earning a Ph.D. in Organic Chemistry in July, 1971. While at Iowa State, the author was a Graduate Research Assistant, Graduate Teaching Assistant, in charge of the Computer Program Library and a Procter and Gamble Summer Fellow.

The author was married to the former Jackie M. Kletter on July 3, 1967.

Since November, 1969, he has been a Postdoctoral Research Associate to Professor J. L. Hoard at Cornell University.